Materials and methods

Mice and parasites

Animal experiments were performed according to the guidelines for animal experimentation of Kyushu University. C57BL/6 mice (female, aged 5 wk) were obtained from Kyudo (Tosu, Japan) and BALB/c nu/nu (nude) mice from CLEA (Japan). IDA mice were bred as described elsewhere [32]. Briefly, C57BL/6 mice, or nude mice, were fed either a control or iron-deficient diet for 10 wk. The diet contained 33% cornstarch, 22% casein, 5% cellulose powder, 30% sucrose, 5% corn oil, 1% AIN-76 vitamin mixture containing 20% choline chloride, 0.02% *p*-aminobenzoic acid, and 4% Harper's mineral mixture without ferric citrate. Ferric citrate, providing 180 mg of iron per kg of final diet, was added to the control diet. Iron-deficient diets contained <10 mg/kg of iron. Mice were housed in plastic cages fitted with stainless steel mesh bottoms to prevent them from ingesting feces.

Blood-stage parasites of *P. yoelii* 17XL (PyL) and *P. yoelii* 17XNL (PyNL) were used in all the experiments (original source: Middlesex Hospital Medical School, University of London 1984). Those two strains have differing virulence, primarily caused by differences in their host cell preference. PyL preferentially invades mature erythrocytes, whereas PyNL mainly infects reticulocytes [15]. Mice were infected intraperitoneally with 25 000 Py-infected erythrocytes obtained from mice freshly inoculated with a frozen stock of the parasites. Parasitemia was checked by Giemsa staining every 2 days and represented as the percentage of parasitized erythrocytes within the total number of erythrocytes.

Hematological analysis

Whole blood was drawn from anesthetized mice by retro-orbital venipuncture. The hemoglobin concentration was measured on the day before challenge by the cyanmethemoglobin method using Drabkin's Reagent (Sigma, St. Louis, MO, USA) according to the manufacturer's instructions [33].

Separation of parasitized erythrocytes

Parasitized erythrocytes were prepared as previously described [34]. Briefly, blood from Py-infected mice was collected with heparin, and passed through a cellulose column to remove WBCs. The RBC solution was placed onto 55% v/v Percoll (Sigma)/PBS and centrifuged and the parasitized erythrocytes at the interface were collected. The purity of the schizonts was usually $>95\%$. The pellets containing ring-infected and uninfected erythrocytes were used as ring stage erythrocytes. In some experiments, parasitized erythrocytes were stained with CSFE (Molecular Probes, Eugene, OR, USA) at 1 μM or 5 μM in PBS) for 20 min at 37°C followed by extensive washing.

In vitro *Plasmodium yoelii* culture

In vitro culture of Py was started at 3% hematocrit, 1–5% parasitized erythrocytes/total RBC, in PRMI-1640 supplemented with 100 IU/mL penicillin, 100 μg/mL streptomycin, 2 mM L-glutamine and 10% inactivated mouse serum. Incubation was carried out under mixed gas consisting of 90% N_2, 5% O_2 and 5% CO_2 at 37°C for 12 h.

ELISA for anti-malaria Abs

Serum from each animal was assayed. Antibodies recognizing Py extracts coated onto Maxisorb plates (Nunc, Roskilde, Denmark) were detected using HRP-conjugated goat anti-mouse IgG or IgG2a, (Zymed Laboratories, San Francisco, CA, USA). Serum samples were run in triplicate and absorbance was read at 405 nm.

Interferon (IFN)-γ ELISA

IFN-γ concentrations were measured in the supernatants from 5×10^5 whole spleen cells 48 h after stimulation with 2 μg/mL of Con A using the mouse IFN-γ Development Kit, Duo Set (R&D Systems, Minneapolis, MN, USA) according to the manufacturer's instructions.

Cell purification and culture

Cell purification was performed using a magnetic cell sorting system (MACS) according to the manufacturer's instructions (Miltenyi Biotech, Bergisch Gladbach, Germany). Mouse spleens were prepared as single cell suspensions. To purify $CD4^+CD25^+$ T cells, the suspensions were incubated with phycoerythrin (PE)-anti-CD25 antibodies (eBioscience, San Diego, CA, USA) followed by anti-PE microbeads (Miltenyi Biotec). $CD4^+CD25^+$ cells were positively selected and used as Tregs. The flow-through cells were incubated with fluorescein isothiocyanate (FITC)-anti-CD4 (eBioscience) followed by anti-FITC microbeads, (Miltenyi Biotec) to yield $CD4^+CD25^-$ T cells. The purity of each cell subset was routinely $>80\%$. Purified $CD4^+$ $CD25^+$ T cells and naïve $CD4^+$ $CD25^-$ T cells were stimulated with Con A at a concentration of 2.5 mg/mL in the presence of APC in 0.2 mL of media (for 72 h) and incubated with 1 Ci/well of $[^3H]$ thymidine for the final 8 h. Radioactivity was measured in a liquid scintillation counter.

Flow cytometry

Single-cell suspensions stained with fluorescence-labeled antibodies were analyzed using a FACSCalibur flow cytometer

(Becton Dickinson, San Jose, CA, USA) and data were analyzed using CellQuest software (Becton Dickinson).

In vitro phagocytosis assays

Inflammatory macrophages were injected into the peritoneal cavity with 4% Brewer's thioglycolate (Difco). Peritoneal exudate cells were harvested 4 days later by peritoneal lavage with complete medium (RPMI containing 5% FBS (Thermo Scientific HyClone, South Logan, UT, USA) 50 mM 2-ME, 2 mM L-glutamine, 100 U/mL penicillin and 100 μg/mL streptomycin). Cells (2×10^5) were plated in 48-well plates, and non-adherent cells were removed after 2 h. The macrophage monolayers were cultured overnight in complete medium. CFSE-labeled parasitized erythrocytes (2×10^6) were then added to the wells. The plates were incubated for 2 h at 37°C. Adherent cells were then detached and analyzed by flow cytometry to assess phagocytosis of labeled cells. Resident splenic macrophages were also used.

Because the ratio of ring-infected erythrocytes differed in each preparation, the clearance of CFSE labeled ring-infected erythrocytes was adjusted according to the following:

Clearance rate of ring-infected erythrocytes = clearance rate of erythrocytes in Percoll pellet × ratio of ring-infected erythrocytes to the total erythrocytes in the pellet.

Measurement of the in vivo clearance of fluorescence-labeled erythrocytes

CSFE-labeled erythrocytes (1×10^7) were injected intravenously into mice. Blood was taken from the mice and the percentage of CFSE-positive erythrocytes estimated by flow cytometry. In some experiments, mice were injected intraperitoneally (i.p.) with 500 μL of CGN at a concentration of 2 mg/mL in PBS once every 2 days. This treatment was started 1 day before infection and continued until the end of each experiment.

Determination of annexin binding to erythrocytes

Suspensions of Py-infected erythrocytes were stained with APC-annexin (BD biosciences) and the DNA dye Syto 16 (Invitrogen, Carlsbad, CA, USA) to detect PS and parasite DNA, respectively. For annexin V binding, erythrocytes were incubated with annexin V for 20 min at room temperature in annexin-binding buffer (140 mM NaCl, 10 mM HEPES, 5 mM glucose, 5 mM $CaCl_2$, pH 7.4). Syto16 (final concentration of 20 nM) was then added to the suspensions followed by incubation for 20 min at room temperature. Cells were then analyzed by flow cytometry.

Measurement of intracellular Ca^{2+}

Intracellular Ca^{2+} measurement was performed as previously described [35] with minor modifications. Packed erythrocytes (2 μL in 2 mL of Ringer's solution (1% Hct)) were loaded with Fluo-4/AM (Invitrogen) by addition of 2 μL of a Fluo-4/AM stock solution (2.0 mM in DMSO). The cells were incubated at 37°C for 15 min with vigorous shaking in a dark room followed by incubation with an additional 2 μM of Fluo-4/AM and 0.2 μg/mL Hoechst 33342 (Molecular Probes) for another 25 min. Cells were then washed twice with Ringer's solution containing 0.5% BSA (Sigma) and once with Ringer's solution alone. As a positive control, erythrocytes were stimulated with 1 μM ionomycin for 3 min prior to analysis to increase intracellular Ca^{2+} activity. Thin blood films were prepared and slides were analyzed using a fluorescence microscope (Keyence, Osaka, Japan).

Statistical analysis

Differences between groups were analyzed for statistical significance using the Mann–Whitney or Wilcoxon tests. For the survival curves, Kaplan–Meier plots and χ^2 tests were used. A p value < 0.05 was considered to be statistically significant.

Acknowledgements: The authors thank Mr. T. Matsumoto, (Keyence Co. Ltd., Osaka, Japan) for technical support in using fluorescence microscopy and the members of the Department of Parasitology, Institutes of Tropical Medicine, Nagasaki University, for support in completing additional experiments. This work was supported by the Ministry of Education, Culture, Sport, Science, and Technology of Japan (Grants 21022036, 20390121).

Conflict of interest: The authors declare no financial or commercial conflict of interest.

References

1 **WHO/UNICEF/UNU.** *Iron deficiency anemia Assessment, Prevention and Control. A Guide for Program Managers.* World Health Organization, Geneva 2001.

2 **de Silva, A., Atukorala, S., Weerasinghe, I. and Ahluwalia, N.,** Iron supplementation improves iron status and reduces morbidity in children with or without upper respiratory tract infection: a randomized controlled studying Colombo Sri Lanka. *Am. J. Clin. Nutr.* 2003. **77**: 234–241.

3 **World malaria report.** World Health Organization, 2009.

4 **Nyakeriga, A. M., Troye-Blomberg, M., Dorfman, J. R., Alexander, N. D., Bäck, R., Kortok, M., Chemtai, A. K. et al.,** Iron Deficiency and malaria among children living on the coast of Kenya. *J. Infect. Dis.* 2004. **190**: 439–447.

5 **Oppenheimer, S. J., Gibson, F. D., Macfarlane, S. B., Moody, J. B., Harrison, C., Spencer, A. and Bunari, O.,** Iron supplementation increases prevalence and effects of malaria: report on clinical studies in Papua New Guinea. *Trans. R. Soc. Trop. Med. Hyg.* 1986. **80**: 603–8012.

6 **Sazawal, S., Black, R. E., Ramsan, M., Chwaya, H. M., Stoltzfus, R. J., Dutta, A., Dhingra, U. et al.,** Effect of routine prophylactic supplementation with iron and folic acid on admission to hospital and mortality in preschool children in a high malaria transmission setting: community-based, randomized, placebo-controlled trial. *Lancet* 2006. **367**:133–143.

7 **Verhoef, H., West, C. E., Nzyuko, S. M., de Vogel, S., van der Valk, R., Wanga, M. A., Kuijsten, A. et al.,** Intermittent administration of iron and sulfadoxine-pyrimethamine to control anemia in Kenyan children: a randomized controlled trial. *Lancet* 2002. **360**: 908–914.

8 **Langhorne, J.,** The immune response to the blood stages of Plasmodium in animal models. *Immunol. Lett.* 1994. **41**: 99–102.

9 **Hisaeda, H., Maekawa, Y., Iwakawa, D., Okada, H., Himeno, K., Kishihara, K., Tsukumo, S. et al.,** Escape of malaria parasites from host immunity requires $CD4^+CD25^+$ regulatory T cells. *Nat. Med.* 2004. **10**: 29–30.

10 **Hisaeda, H., Tetsutani, K., Imai, T., Moriya, C., Tu, L., Hamano, S., Duan, X. et al.,** Malaria parasites require TLR9 signaling for immune evasion by activating regulatory T cells. *J. Immunol.* 2008. **180**: 2496–2503.

11 **Coban, C., Ishii, K. J., Kawai, T., Hemmi, H., Sato, S., Uematsu, S., Takeuchi, O. et al.,** Toll-like receptor 9 mediates innate immune activation by the malaria pigment hemozoin. *J. Exp. Med.* 2005. **201**: 19–25.

12 **Bastos, K. R., Barboza, R., Elias, R. M., Sardinha, L. R., Grisotto, M. G., Marinho, C. R., Amarante-Mendes, G. P. et al.,** Impaired macrophage responses may contribute to exacerbation of blood-stage Plasmodium chabaudi chabaudi malaria in interleukin-12-deficient mice. *J. Interferon Cytokine Res.* 2002. **22**: 1191–1199.

13 **Koka, S., Föller, M., Lamprecht, G., Boini, K. M., Lang, C., Huber, S. M. and Lang, F.,** Iron deficiency influences the course of malaria in *Plasmodium berghei* infected mice. *Biochem. Biophys. Res. Commun.* 2007. **357**: 608–614.

14 **Bosman, G. J., Willekens, F. L. and Were, J. M.,** Erythrocyte aging: a more than superficial resemblance to apoptosis? *Cell. Physiol. Biochem.* 2005. **16**: 1–8.

15 **Hargreaves, J., Yoeli, M. and Nussenzweig, R. S.,** Immunological studies in rodent malaria I: Protective immunity induced in mice by mild strains of Plasmodium berghei yoelii against a virulent and fatal line of this plasmodium. *Ann. Trop. Med. Parasitol.* 1975. **69**: 289–299.

16 **Leida, M. N., Mahoney, J. R. and Eaton, J. W.,** Intraerythrocytic plasmodial calcium metabolism. *Biochem. Biophys. Res. Commun.* 1981. **103**: 402–406.

17 **Goma, J., Renia, L., Miltgen, F. and Mazier, D.,** Effect of iron deficiency on the hepatic development of *Plasmodium yoelii*. *Parasite* 1995. **2**: 351–356.

18 **Lewis-Hughes, P. H. and Howell, M. J.,** In vitro culture of *Plasmodium yoelii* blood stage. *Inter. J. Parasitol.* 1984. **14**: 447–451.

19 **Luzzi, G. A., Torii, M., Aikawa, M. and Pasvol, G.,** Unrestricted growth of *Plasmodium falciparum* in microcytic erythrocytes in iron deficiency and thalassaemia. *Br. J. Haematol.* 1990. **74**: 519–524.

20 **Fadok, V. A., Bratton, D. L., Rose, D. M., Pearson, A., Ezekewitz, R. A. and Henson, P. M.,** A receptor for phosphatidylserine-specific clearance of apoptotic cells. *Nature* 2000. **405**: 85–90.

21 **López-Revuelta, A., Sánchez-Gallego, J. I., García-Montero, A. C., Hernández-Hernández, A., Sánchez-Yagüe, J. and Llanillo, M.,** Membrane cholesterol in the regulation of aminophospholipid asymmetry and phagocytosis in oxidized erythrocytes. *Free Radic. Biol. Med.* 2007. **42**: 1106–1118.

22 **Miki, Y., Tazawa, T., Hirano, K., Matsushima, H., Kumamoto, S., Hamasaki, N., Yamaguchi, T. et al.,** Clearance of oxidized erythrocytes by macrophage: Involvment of caspases in the generation of clearance signal at band 3 glycoprotein. *Biochem. Biophys. Res. Commun.* 2007. **363**: 57–62

23 **Orrenius, S., Zhivotovsky, B. and Nicotera, P.,** Regulation of cell death: The calcium-apoptosis link. *Nat. Rev. Mol. Cell. Biol.* 2003. **7**: 552–565.

24 **Mandal, D., Mazumder, A., Das, P., Kundu, M., Basu, J.,** Fas-, caspase 8-, and caspase 3-dependent signaling regulates the activity of the aminophospholipid translocase and phosphatidylserine externalization in human erythrocytes. *J. Biol. Chem.* 2005. **280**: 39460–39467.

25 **Föller, M., Huber, S. M., Lang, F.,** Erythrocyte programmed cell death. *IUBMB Life* 2008. **60**: 661–668.

26 **Huang, C. J., Gurlo, T., Haataja, L., Costes, S., Daval, M., Ryazantsev, S., Wu, X. et al.,** Calcium-activated calpain-2 is a mediator of beta cell dysfunction and apoptosis in type 2 diabetes. *J. Biol. Chem.* 2010. **285**: 339–348.

27 **Cook, J. D. and Lynch, S. R.,** The liabilities of iron deficiency. *Blood* 1986. **68**: 803–809.

28 **Kleinclauss, F., Perruche, S., Masson, E., de Carvalho Bittencourt, M., Biichle, S., Remy-Martin, J. P., Ferrand, C. et al.,** Intravenous apoptotic spleen cell infusion induces a TGF-beta-dependent regulatory T-cell expansion. *Cell Death Differ.* 2006. **13**: 41–52.

29 **Ayi, K., Turrini, F., Piga, A. and Arese, P.,** Enhanced phagocytosis of ring-parasitized mutant erythrocytes: a common mechanism that may explain protection against falciparum malaria in sickle trait and beta-thalassemia trait. *Blood* 2004. **104**: 3364–3371.

30 **Cappadoro, M., Giribaldi, G., O'Brien, E., Turrini, F., Mannu, F., Ulliers, D. and Simula, G.,** Early phagocytosis of glucose-6-phosphate dehydrogenase (G6PD)-deficient erythrocytes parasitized by Plasmodium falciparum may explain malaria protection in G6PD deficiency. *Blood* 1998. **92**: 2527–2534.

31 **Min-Oo, G. and Gros, P.,** Erythrocyte variants and the nature of their malaria protective effect. *Cell. Microbiol.* 2005. **92**: 753–763.

32 **Harvey, P. W., Bell, R. G., Nesheim, M. C.,** Iron deficiency protects inbred mice against infection with Plasmodium chabaudi. *Infect. Immun.* 1985. **50**: 932–934

33 **DeMaeyer, E. M., Dallman, P., Gurney, J. M., Hallberg, L., Sood, S. K. and Srikantia, S. G.,** *Preventing and controlling iron deficiency anaemia through primary health care.* World Health Organization, Geneva 1989.

34 **Urban, B. C., Ferguson, D. J., Pain, A., Willcox, N., Plebanski, M., Austyn, J. M. and Roberts, D. J.,** *Plasmodium falciparum*-infected erythrocytes modulate the maturation of dendritic cells. *Nature* 1999. **400**: 73–77.

35 **Kempe, D. S. and Lang, F.,** Enhanced programmed cell death of iron-deficiency erhyrocytes. *FASEB J.* 2005. **20**: 368–370.

Abbrevations: **APT:** aminophospholipid translocase · **CGN:** carrageenan · **IDA:** iron deficiency anemia · **PS:** phosphatidylserine · **Py:** *Plasmodium yoelii*

Full correspondence: Dr. Hajime Hisaeda, Department of Parasitology, Graduate School of Medicine, Gunma University, 3-39-22 Showa-machi, Maebashi, Gunma 371-8511, Japan
Fax: +81-27-220-8025
e-mail: hisa@med.gunma-u.ac.jp

Received: 10/9/2010
Revised: 2/2/2011
Accepted: 23/2/2011
Accepted article online: 1/3/2011

ISSN (Print) 0023-4001
ISSN (Online) 1738-0006

Korean J Parasitol. Vol. 49, No. 1: 85-90, March 2011
DOI: 10.3347/kjp.2011.49.1.85

▣ BRIEF COMMUNICATION

CD8+ T-cell Activation in Mice Injected with a Plasmid DNA Vaccine Encoding AMA-1 of the Reemerging Korean *Plasmodium vivax*

Hyo-Jin Kim[1,†], Bong-Kwang Jung[1,†], Jin-Joo Lee[1], Kyoung-Ho Pyo[1], Tae Yun Kim[2], Byung-il Choi[3], Tae Woo Kim[4], Hajime Hisaeda[5], Kunisuke Himeno[6], Eun-Hee Shin[1,7] and Jong-Yil Chai[1,*]

[1]Department of Parasitology and Tropical Medicine, Seoul National University College of Medicine, and Institute of Endemic Disease, Seoul National University Medical Research Center, Seoul 110-799, Korea; [2]Department of Environmental Medical Biology, Yonsei University College of Medicine, Seoul 120-752, Korea; [3]Department of Anatomy, College of Medicine, Korea University, Brain Korea 21, Seoul 136-705, Korea; [4]Divison of Infection and Immunology, Graduate School of Medicine, Korea University, Seoul 136-701, Korea; [5]Department of Parasitology, Graduate School of Medicine, Gunma University, Maebashi 371-8581, Japan; [6]Department of Parasitology, Graduate School of Medical Sciences, Kyushu University, Fukuoka 812-8582, Japan; [7]Seoul National University Bundang Hospital, Seongnam 463-707, Korea

Abstract: Relatively little has been studied on the AMA-1 vaccine against *Plasmodium vivax* and on the plasmid DNA vaccine encoding *P. vivax* AMA-1 (PvAMA-1). In the present study, a plasmid DNA vaccine encoding AMA-1 of the reemerging Korean *P. vivax* has been constructed and a preliminary study was done on its cellular immunogenicity to recipient BALB/c mice. The PvAMA-1 gene was cloned and expressed in the plasmid vector UBpcAMA-1, and a protein band of approximately 56.8 kDa was obtained from the transfected COS7 cells. BALB/c mice were immunized intramuscularly or using a gene gun 4 times with the vaccine, and the proportions of splenic T-cell subsets were examined by fluorocytometry at week 2 after the last injection. The spleen cells from intramuscularly injected mice revealed no significant changes in the proportions of CD8+ T-cells and CD4+ T-cells. However, in mice immunized using a gene gun, significantly higher ($P<0.05$) proportions of CD8+ cells were observed compared to UB vector-injected control mice. The results indicated that cellular immunogenicity of the plasmid DNA vaccine encoding AMA-1 of the reemerging Korean *P. vivax* was weak when it was injected intramuscularly; however, a promising effect was observed using the gene gun injection technique.

Key words: *Plasmodium vivax*, DNA vaccine, apical membrane antigen (AMA), CD8+ T-cell, gene gun

Intramuscular or gene gun-based injections of plasmid DNA expression vectors, i.e., DNA vaccines, induce corresponding protein expression in vivo and generate humoral and cellular immune responses against various infectious agents [1]. DNA vaccines are simple, inexpensive, and heat-stable, and can induce protective immunity without using live organisms, replicating vectors, or harmful adjuvants [2]. Significant progress has recently been made in the development of malaria DNA vaccines targeting the pre-erythrocytic and erythrocytic stage antigens. Circumsporozoite proteins (CSP), merozoite surface proteins (MSP), Duffy-binding protein (DBP), and apical membrane antigens (AMA) have been used as antigens [2-4].

• Received 21 December 2010, revised 3 February 2011, accepted 3 February 2011.
† These authors contributed equally to this study.
*Corresponding author (cjy@snu.ac.kr)

Apical membrane antigen 1 (AMA-1), previously known as *Pf*83 and *Pk*66 in *Plasmodium falciparum*, is a micronemal protein of apicomplexan parasites and is essential during the invasion of malarial parasites into host cells [5]. There is a single gene for this antigen in all *Plasmodium* species [5]. AMA-1 is a good vaccine candidate because it can have profound parasite-inhibitory effects in vitro and in animal models [5]. Several studies have examined the vaccine potential of AMA-1 against *P. falciparum* and other human-infecting malaria [6,7]. However, relatively little has been studied on AMA-1 vaccines against *Plasmodium vivax* [8,9].

Since important issues were raised about *P. vivax*, including its global burden, drug resistance, severity of the disease, prevalence of relapse and recrudescence, and problems of coinfection with *P. falciparum*, there is a renewed interest in the development of a *P. vivax* vaccine [10]. A modest number of *P. vivax* vaccine candidates, including CSP, MSP, and DBP, have been tested in pre-clinical trials in rodents [11], and several CSPs and

an ookinete surface antigen (Pvs25) were assessed in phase I clinical trials [10]. Vaccination with *P. vivax* AMA-1 (PvAMA-1) was attempted in primates [8], and PvAMA-1 was shown to elicit differentiation of dendritic cells in naturally infected vivax malaria patients [9]. However, few studies have been reported on plasmid DNA vaccines encoding PvAMA-1 [3]. The present study aimed to construct a DNA plasmid vaccine encoding AMA-1 of the reemerging *P. vivax* in the Republic of Korea (= Korea), and to preliminarily observe its cellular immunogenicity in recipient BALB/c mice.

Six-week-old female BALB/c mice (Koatech, Pyeongtaek, Gyeonggi-do, Korea) were supplied with food and water sterilized by irradiation and autoclaving. All animal procedures were performed according to the approved protocols and institutional recommendations for the proper use and care of laboratory animals, Seoul National University College of Medicine.

Blood samples were collected from 17 *P. vivax* patients (designated SKPV1 through SKPV17) diagnosed at the Department of Parasitology and Tropical Medicine, Seoul National University College of Medicine, Seoul, and Paju Medical Center, Paju, Gyeonggi-do (Province), Korea between 1995 and 2000, and frozen at -80°C. The level of parasitemia ranged from 500 to 6,200 parasites per μl blood. The genomic DNA of *P. vivax* was extracted using the QIAmp DNA Mini kit (Qiagen, Hilden, Germany). After ethanol precipitation, it was dissolved in distilled water and kept at -80°C. After PCR amplification of AMA-1, its nucleotide sequences were compared with those of the Salvador strain (Sal-1) (GenBank accession number; AF063138). The primer sets were based on the oligonucleotide sequences of PvAMA-1 [12]. One μl of genomic DNA and 20 *p*mol each of forward and reverse primers were added to the PCR premix (Bioneer, Seoul, Korea). The PCR products were amplified in 35 cycles using a GeneAmp PCR System 9600 DNA thermal cycler (PE Applied Biosystems, Forster City, California, USA). The PCR conditions were as follows: denaturation at 95°C for 1 min, annealing at the indicated temperature for 1 min, and extension at 72°C for 1 min. The DNA band visualized by ethidium bromide staining after electrophoresis was extracted using the QIAEX II gel extraction kit (Qiagen).

The PCR products of AMA-1 were subcloned using the pCR2.1 cloning vector of a TOPO Cloning Kit (Invitrogen, Carlsbad City, California, USA). *Escherichia coli*, strain JM109, was used as the host for transformation. When target fragments from positive clones were confirmed, the plasmid was prepared using the miniprep kit (Qiagen) and sequenced using a model ABI Prime 377 Automatic Sequencer (PE Applied Bio-systems). The gene UBpcDNA encoding the mutant ubiquitin, whose C-terminal Gly residue was replaced by Ala (G74A), originated in the liver of BALB/c mice and was inserted into the *Nhe I* and *Xho I* sites of pcDNA 3.1(-) vector, which was supplied by the Department of Parasitology, Graduate School of Medical Sciences, Kyushu University, Japan [13].

For construction of UBpcAMA-1, the miniprep products of the DNA-TA vector for AMA-1 were digested with *Xho I* and *Apa I* enzymes, and ligated to the 3' of the gene encoding mutant ubiquitin cDNA in the frame and inserted into the *Apa I* site of pcDNA3.1(-) attached C-terminal His tag (Fig. 1A). AMA-1 protein expression in COS7 cells (Korea Cell Line Bank, Seoul, Korea) transfected with UBpcAMA-1 plasmid was confirmed by immunofluorescence stain (Fig. 1B) and western blot (Fig. 1C). COS7 cells were cultured in DMEM medium supplemented with 10% FBS (GIBCO BRL, Grand Island, New York, USA) in a 5% humidified CO_2 incubator at 37°C. At 24 hr after the transfection, 10 μM MG132, an inhibitor of proteasomes, was used and, at 48 hr, cells were harvested and lysed by the addition of 200 μl lysis buffer.

DNA vaccine injection was performed either intramuscularly (10 μg vaccine in 100 μl saline) into the quadriceps muscle or with a gene gun into the epidermis [2]. Mice, 3-5 in each group, were anesthetized with sodium pentobarbital (75 mg/kg) and vaccinated a total of 4 times at 2 week intervals. For gene gun injection, the expression plasmid was precipitated onto 1.6 mm diameter gold particles (12.5 mg particles in 100 μl 0.05 M spermidine mixed with 100 μl of 100 μg plasmid), and the plasmid-gold particles were resuspended in 6 ml of ethanol and coated onto the inner surface of a tube. The plasmid DNA was delivered to the shaved abdominal skin of mice in 1 shot using the Helios Gene Gun (Bio-Rad, Hercules, California, USA) at a helium pressure of 300 p.s.i. For comparison, groups of mice were immunized with 2 μg UB vector (control group), 2 μg UBpcAMA-1 (AMA-1 group), 1 μg UBpcAMA-1 plus 1 μg UBpcIL-12 (AMA-1 + IL-12 group), or 2 μg UBpcIL-12 (IL-12 group) per shot.

Phenotype changes of splenocytes before and after vaccination were examined using flow cytometry at 2 weeks after the final boosting. Spleens were removed and gently crushed through a stainless steel mesh. After lysis of erythrocytes and washing for 10 min at 1,500 rpm, splenocytes were suspended in complete RPMI 1640 media. For fluorescence-activated cell sorter

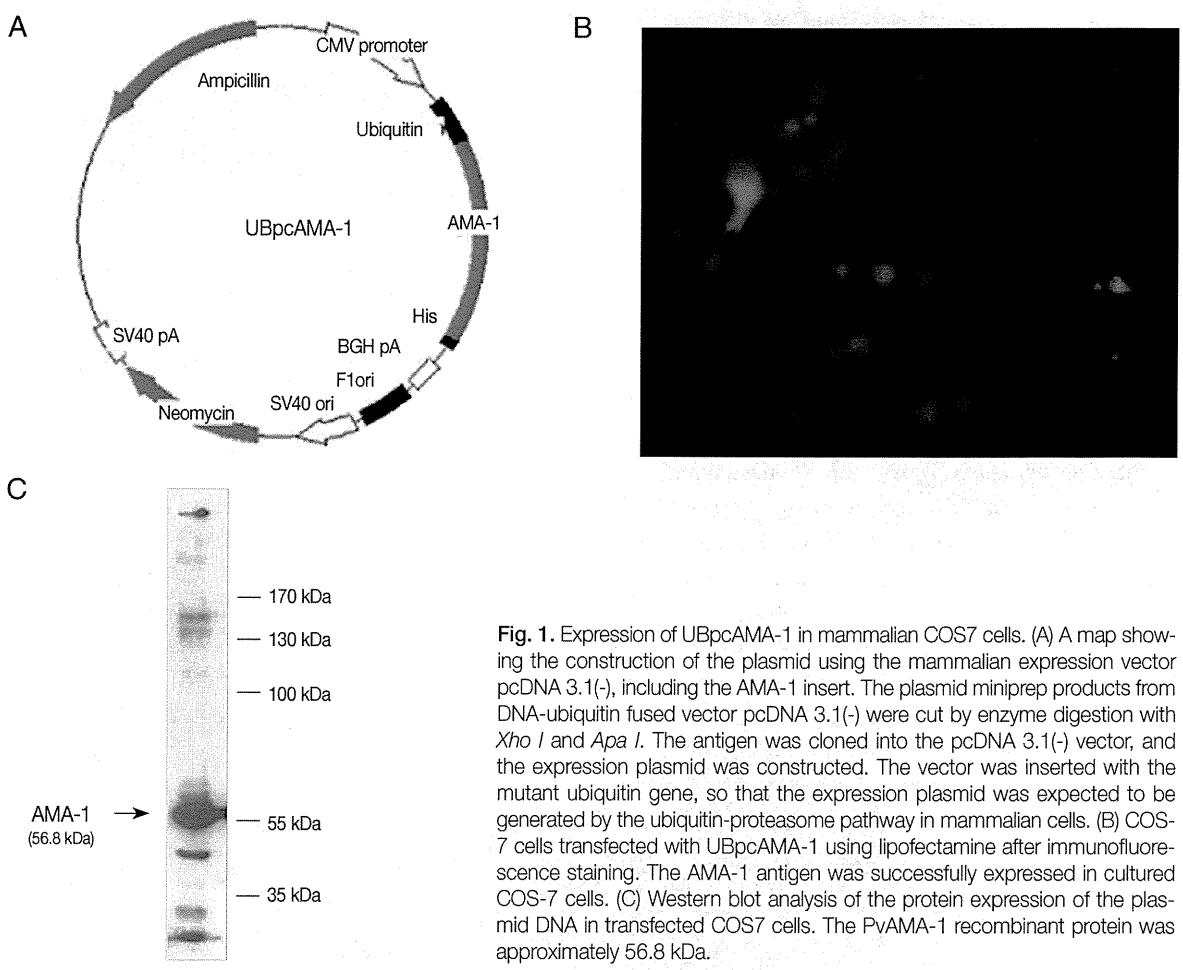

Fig. 1. Expression of UBpcAMA-1 in mammalian COS7 cells. (A) A map showing the construction of the plasmid using the mammalian expression vector pcDNA 3.1(-), including the AMA-1 insert. The plasmid miniprep products from DNA-ubiquitin fused vector pcDNA 3.1(-) were cut by enzyme digestion with *Xho I* and *Apa I*. The antigen was cloned into the pcDNA 3.1(-) vector, and the expression plasmid was constructed. The vector was inserted with the mutant ubiquitin gene, so that the expression plasmid was expected to be generated by the ubiquitin-proteasome pathway in mammalian cells. (B) COS-7 cells transfected with UBpcAMA-1 using lipofectamine after immunofluorescence staining. The AMA-1 antigen was successfully expressed in cultured COS-7 cells. (C) Western blot analysis of the protein expression of the plasmid DNA in transfected COS7 cells. The PvAMA-1 recombinant protein was approximately 56.8 kDa.

(FACS) analysis, cells were adjusted to 1×10^7 cells per ml, and 100 µl (1×10^6 cells) of this cell suspension was stained with specific antibodies. To avoid non-specific binding, purified rat anti-mouse CD16/32 (Fcγ III/II receptor) mAb (eBioscience, San Diego, California, USA) was added before labeling with specific antibodies. For phenotype determination, the following mAbs were used: fluorescein isothiocyanate-conjugated anti-mouse mAb against CD3⁺ T-cells (CD3e, clone 145-2C11) (eBioscience), Cy5-conjugated anti-mouse mAb against CD8⁺ T-cells (CD8a LY-2, clone 53-6.7) (eBioscience), and PE-conjugated anti-mouse mAb against CD4⁺ T-cells (CD4 L3T4, clone GK1.5) (eBioscience). Fluorescence was quantified using BD FACS Calibur Flow Cytometer (BD science, San Jose, New Jersey, USA).

Data were compared using the Mann-Whitney U test (SPSS Inc., Chicago, Illinois, USA) which is appropriate for testing small numbers of samples. A *P*-value of < 0.05 was considered statistically significant.

Little polymorphism was observed in PvAMA-1 gene among the 17 reemerging Korean isolates (data not shown). Also, the nucleotide sequence of SKPV1, one of the 17 isolates, showed over 99% homology with other previously reported Korean isolates (SK-G, SK-A, SKOR-67, SKOR-68) and over 98% homology with foreign strains, Sal-1 (El Salvador) and PH-84 (the Philippines) (data not shown). The amino acid sequence homology was over 97% with Sal-1, over 98% with SK-G, SKOR-67, SKOR-68, and PH-84, and over 99% with SK-A.

The eukaryotic expression plasmid, UBpcAMA-1, was constructed as described in Fig. 1A. The mammalian expression vector, pcDNA 3.1(-), was inserted with AMA-1 and mutant ubiquitin genes, and thus the expression plasmid was generated by the ubiquitin-proteasome pathway in mammalian cells.

The plasmid miniprep products from DNA-ubiquitin fused vector pcDNA 3.1(-) were cut by digestion with *Xho I* and *Apa I* enzymes. The DNA fragments of PCR products were subcloned into TA vectors and the genes encoding these antigens were sequenced. Then, the antigens were cloned into the pcDNA 3.1(-) vector and the expression plasmids were constructed (Fig. 1A). Immunofluorescence staining revealed brilliant cytoplasmic expression of AMA-1 in COS7 cells transfected with UBpcAMA-1 plasmid (Fig. 1B). We also confirmed the expression of expected proteins by western blot analysis. The immunoblots showed a large protein band of about 56.8 kDa present in COS7 cells transfected with UBpcAMA-1 (Fig. 1C).

The spleens of intramuscularly or gene gun immunized mice enlarged notably compared with those of the unimmunized controls. In particular, the spleen weight of the gene gun injected mice almost doubled that of the unimmunized controls (data not shown). FACS analysis of spleen cells harvested 2 weeks after the final immunization with AMA-1 or AMA-1 plus IL-12 DNA vaccines showed notable differences in the proportions of $CD4^+$ and $CD8^+$ T-lymphocytes between the intramuscular injection versus the gene gun (epidermis) injection (Fig. 2). In mice immunized intramuscularly (n=5 for each group) with AMA-1 alone or AMA-1 plus IL-12 DNA vaccines, the proportions of T-cell subsets (17.9±0.47% or 15.5±0.79% for $CD8^+$ T-cells and 27.6±0.84% or 27.7±0.72% for $CD4^+$ T-cells) did not show any significant changes ($P>0.05$), compared with control mice immunized only with UB vector (16.2±0.78% for $CD8^+$ T-cells and 26.5±0.35% for $CD4^+$ T-cells) (Fig. 2). By contrast, in mice injected with a gene gun (n=3 for each group), significantly higher proportions of $CD8^+$ T-cells were found in those immunized with AMA-1, IL-12, or AMA-1 plus IL-12 DNA vaccines (24.9±0.44%, 20.8±0.61, or 24.2±1.56%, respectively), compared with control mice immunized only with UB vector (19.2±0.66%) (Fig. 2). However, even in mice injected with a gene gun, the proportions of $CD4^+$ T-cells did not change significantly in AMA-1 alone or AMA-1 plus IL-12 injection groups (28.1±5.66% or 36.9±4.76%, respectively), compared with control mice immunized with UB vector (30.3±0.55%) (Fig. 2).

In the reemerging vivax malaria in Korea, little polymorphism has been found in 18S rRNA [14] and AMA-1 [15,16] but a considerable degree of variation has been found on merozoite surface protein-3α [17]. Control programs have been in operation but no vaccine development has been reported. To our knowledge, this is the first report of a vaccine candidate targeting the reemerging vivax malaria in Korea.

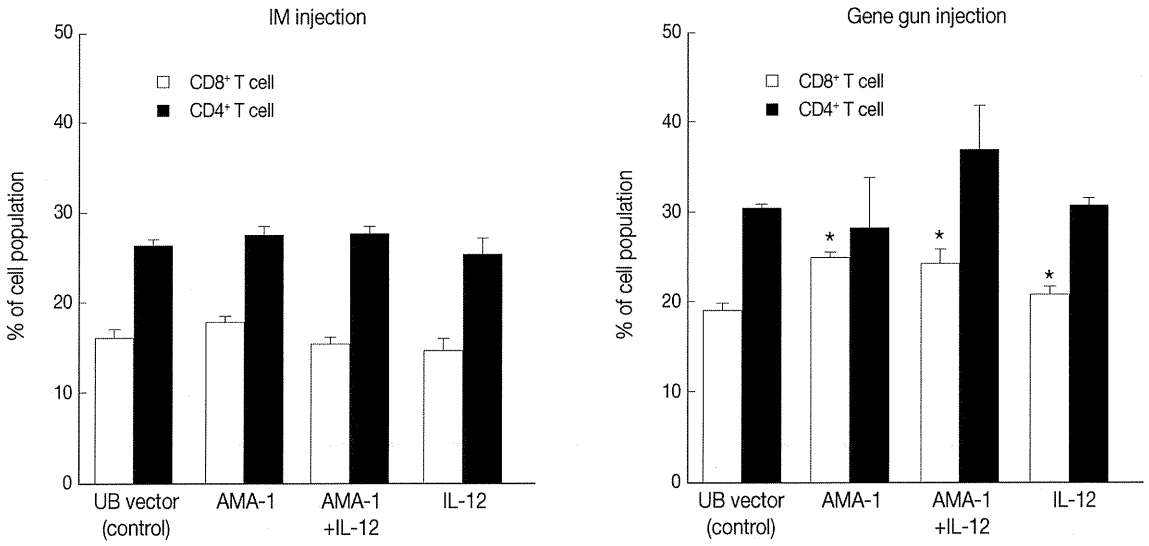

Fig. 2. Changes of $CD8^+$ and $CD4^+$ T-lymphocyte population in PvAMA-1 DNA vaccine-immunized mice by intramuscular (IM) or gene gun injection methods. Immunization was performed a total of 4 times at 2 weeks interval with PvAMA-1 DNA vaccine alone or in combination with IL-12 DNA vaccine (n=5 mice for IM and n=3 for gene gun injection). Splenocytes were harvested 2 weeks after the final immunization and changes of $CD4^+$ and $CD8^+$ T-lymphocyte proportions were determined by flow cytometric analysis. Significant increases ($P<0.05$) of $CD8^+$ T-cell populations were found in PvAMA-1 DNA vaccine alone and PvAMA-1 plus IL-12 DNA vaccine immunized groups compared with the controls injected with the gene gun.

The AMA-1 of *P. vivax* and *P. falciparum* has 3 extracellular domains (designated domains I, II, and III in N- to C-terminal order) [18]. The AMA-1 of *P. vivax* can have significant nucleotide sequence polymorphism at domain I, as seen in Myanmar isolates [19]. However, PvAMA-1 has little polymorphism at domain II, and has, therefore, been highlighted as a potential vaccine candidate [20]. The AMA-1 of the reemerging Korean *P. vivax* isolates has 2 genotypes and show little polymorphism [15,16]. The present study also revealed little genetic polymorphism in the PvAMA-1 of the reemerging Korean isolates. The sequence was over 98-99% homologous to the previously reported Korean (SK-A, SK-G, SKOR-67, and SKOR-68) or foreign isolates (Sal-1, PH-84, CH-05A, CH-10A, PNG, and INDO) [15, 16]. Therefore, we considered that PvAMA-1 DNA vaccine is a potential vaccine candidate for the reemerging Korean *P. vivax*.

To confirm in vitro expression of AMA-1, we selected a eukaryotic expression system using COS7 mammalian cells for transfection with the plasmid vector UBpcAMA-1. Ubiquitin was used to fuse AMA-1 with the vector [13]. In this vector, mutant ubiquitin was expected to conduct antigen presentation to MHC class I molecules and to activate $CD8^+$ T-cells [21]. In our study, ubiquitin-fused AMA-1 was successfully expressed after using a proteasome inhibitor, MG132, and confirmed as a 56.8 kDa protein by western blotting.

Despite the advantages of plasmid DNA vaccines, their applicability is generally limited by their poor immunogenicity and protective capacity [3]. One of the factors influencing the poor immunogenicity of DNA vaccines is a lowered efficacy of antigen expression [4]. Genes cloned from a pathogenic organism may not be efficiently translated in a heterologous host expression system as a consequence of codon bias displayed between different species [4]. One potential approach to enhance the immunogenicity of plasmid DNA vaccines is to maximize pathogenic protein expression by changing the codon usage of the gene of interest to reflect that of the gene of the transfected mammalian host cells [4,22,23]. In *P. falciparum* CSP, *P. yoelii* CSP, and *P. yoelii* hepatocyte erythrocyte protein (PyHEP17) DNA vaccine models, mammalian codon optimization enhanced expression of target proteins in vitro and antibody responses in immunized mice. However, codon optimization did not enhance T-cell responses or protective immunity [4]. The effect of codon optimization of DNA vaccines may vary depending on the antigen, pathogen, or host system, and should be tested on a case-by-case basis. In our study, we did not use codon optimization.

An important result of our preliminary study was that immunogenicity of PvAMA-1 DNA vaccine differed between intramuscular and gene gun immunization methods and that the gene gun immunization resulted in enhanced $CD8^+$ T-cell responses of recipient mice. This result was in accordance with previous reports on a plasmid DNA vaccine encoding a cytotoxic T-lymphocyte epitope or ovalbumin (OVA) [24] and a DNA vaccine expressing a hemagglutinin antigen from an H5-N1 influenza virus [25]. The gene gun method resulted in more reliable and reproducible results than the intramuscular injection method for DNA vaccination in inducing effective and consistent immune responses in animal models [24,25]. The difference in reproducibility may be related to the difference in antigen presentation mechanisms between the 2 methods [23]. In the gene gun system, the plasmid DNA is injected into the epidermis where the most important antigen presenting cells are epidermal dendritic cells (Langerhans cells). In the muscle, myocytes do not work as primary antigen presenting cells [22].

We regret that the actual cell numbers of different T-cell phenotypes in the mouse spleen were not obtained in fluorocytometric analyses. However, we observed that the spleens of immunized mice were enlarged, without exception, compared to the unimmunized controls. Therefore, it is for sure that the significant increases of $CD8^+$ T-cell proportions represent substantial increases in the actual numbers of $CD8^+$ T-cells in the immunized mice.

Conclusively, in our study, a plasmid DNA vaccine encoding AMA-1 of the reemerging Korean *P. vivax* has been successfully constructed and significantly higher ($P<0.05$) proportions of splenic $CD8^+$ cells were observed in mice subcutaneously immunized using a gene gun compared to UB vector-injected non-immunized controls. Further studies on the efficacy of the gene gun technique will be useful for the development of *P. vivax* DNA vaccines.

ACKNOWLEDGEMENTS

This work was supported by Seoul National University Bundang Hospital Research Fund no. 02-2007-008 (2007) and Seoul National University Hospital Grant no. 04-2008-0920 (2008).

REFERENCES

1. Gurunathan S, Klinman DM, Seder RA. DNA vaccines: Immu-

nology, application, and optimization. Annu Rev Immunol 2000; 18: 927-979.
2. Sakai T, Hisaeda H, Nakano Y, Zhang M, Takashima M, Ishii K, Maekawa Y, Matsumoto S, Nitta Y, Miyazaki J, Yamamoto S, Himeno K. Gene gun-based co-immunization of merozoite surface protein-1 cDNA with IL-12 expression plasmid confers protection against lethal *Plasmodium yoelii* in A/J mice. Vaccine 2003; 21: 1432-1444.
3. Rogers WO, Gowda K, Hoffman SL. Construction and immunogenicity of DNA vaccine plasmids encoding four *Plasmodium vivax* candidate vaccine antigens. Vaccine 1999; 17: 3136-3144.
4. Dobaño C, Sedegah M, Rogers WO, Kumar S, Zheng H, Hoffman SL, Doolan D. *Plasmodium*: Mammalian codon optimization of malaria plasmid DNA vaccines enhances antibody responses but not T cell responses nor protective immunity. Exp Parasitol 2009; 122: 112-123.
5. Remarque EJ, Faber BW, Kocken CHM, Thomas AW. Apical membrane antigen 1: A malaria vaccine candidate in review. Trends Parasitol 2008; 24: 74-84.
6. Kusi KA, Faber BW, Thomas AW, Remarque EJ. Humoral immune response to mixed PfAMA1 alleles; multivalent PfAMA1 vaccines induce broad specificity. PLOS One 2009; 4: e8110.
7. Dutta S, Sullivan JS, Grady KK, Haynes JD, Komisar J, Batchelor AH, Soisson L, Diggs CL, Heppner DG, Lanar DE, Collins WE, Barnwell JW. High antibody titer against apical membrane antigen-1 is required to protect against malaria in the Aotus model. PLOS One 2009; 4: e8138.
8. Kocken CHM, Dubbeld MA, Van Der Wel A, Pronk JT, Waters AP, Langermans JAM, Thomas AW. High-level expression of *Plasmodium vivax* apical membrane antigen 1 (AMA-1) in *Pichia pastoris*: Strong immunogenicity in *Macaca mulatta* immunized with *P. vivax* AMA-1 and adjuvant SBAS2. Infect Immun 1999; 67: 43-49.
9. Bueno LL, Morais CG, Soares IDS, Bouillet LEM, Bruna-Romero O, Fontes CJ, Fujiwara RT, Braga EM. *Plasmodium vivax* recombinant vaccine candidate AMA-1 plays an important role in adaptive immune response eliciting differentiation of dendritic cells. Vaccine 2009; 27: 5581-5588.
10. Herrera S, Corradin G, Arévalo-Herrera M. An update on the search for a *Plasmodium vivax* vaccine. Trends Parasitol 2007; 23: 122-128.
11. World Health Organization. Update on development of vaccines against *Plasmodium vivax* malaria (http://www.who.int/vaccines-documents). 2005.
12. Rodriguez MHC, Rodriguez KM, Oliveira TR, Cômodo AN, Rodriguez MM, Kocken CHM, Thomas AW, Soares IS. Antibody response of naturally infected individuals to recombinant *Plasmodium vivax* apical membrane antigen-1. Int J Parasitol 2005; 35: 185-192.
13. Zhang M, Obata C, Hisaeda H, Ishii K, Murata S, Chiba T, Chiba T, Tanaka K, Li Y, Furue M, Chou B, Imai T, Duan X, Himeno K. A novel DNA vaccine based on ubiquitin-proteasome pathway targeting 'self'-antigens expressed in melanoma/melanocyte. Gene Therapy 2005; 12: 1049-1057.
14. Chai JY, Park YK, Guk SM, Oh KH, Oh MD, Lee SH, Kim HS, Wataya Y. trial for a DNA diagnosis of *Plasmodium vivax* malaria recently reemerging in the Republic of Korea using microtiter plate hybridization assay. Am J Trop Med Hyg 2000; 63(1-2): 80-84.
15. Han ET, Park JH, Shin EH, Choi MH, Oh MD, Chai JY. Apical membrane antigen-1 (AMA-1) gene sequences of re-emerging *Plasmodium vivax* in South Korea. Korean J Parasitol 2002; 40: 157-162.
16. Chung JY, Chun EH, Chun JH, Kho WG. Analysis of the *Plasmodium vivax* apical membrane antigen-1 gene from re-emerging Korean isolates. Parasitol Res 2003; 90: 325-329.
17. Han ET, Song TE, Park JH, Shin EH, Guk SM, Kim TY, Chai JY. Allelic dimorphism in the merozoite surface protein-3alpha in Korean isolates of *Plasmodium vivax*. Am J Trop Med Hyg 2004; 71: 745-749.
18. Pizarro JC, Vulliez-Le Normand B, Chesne-Seck ML, Collins CR, Withers-Martinez C, Hackett F, Blackman MJ, Faber BW, Remarque EJ, Kocken CHM, Thomas AW, Bentley GA. Crystal structure of the malaria vaccine candidate apical membrane antigen 1. Science 2005; 308: 408-411.
19. Moon SU, Na BK, Kang JM, Kim JY, Cho SH, Park YK, Sohn WM, Lin K, Kim TS. Genetic polymorphism and effect of natural selection at domain I of apical membrane antigen-1 (AMA-1) in *Plasmodium vivax* isolates from Myanmar. Acta Trop 2010; 114: 71-75.
20. Putaporntip C, Jongwutiwes S, Grynberg P, Cui L, Hughes AL. Nucleotide sequence polymorphism at the apical membrane antigen-1 locus reveals population history of *Plasmodium vivax* in Thailand. Infect Genet Evol 2009; 9: 1295-1300.
21. Kloetzel PM. Antigen processing by the proteasome. Nat Rev Mol Cell Biol 2001; 2: 179-187.
22. Narum DL, Kumar S, Rogers WO, Fuhrmann SR, Liang H, Oakley M, Taye A, Sim BKL, Hoffman SL. Codon optimization of gene fragments encoding *Plasmodium falciparum* merozoite proteins enhances DNA vaccine protein expression and immunogenicity in mice. Infect Immun 2001; 69: 7250-7253.
23. Yazdani SS, Shakri AR, Pattnaik P, Rizvi MMA, Chitnis CE. Improvement in yield and purity of a recombinant malaria vaccine candidate based on the receptor-binding domain of *Plasmodium vivax* Duffy binding protein by codon optimization. Biotechnol Lett 2006; 28: 1109-1114.
24. Yoshida A, Nagata T, Uchijima M, Higashi T, Koide Y. Advantage of gene gun-mediated over intramuscular inoculation of plasmid DNA vaccine in reproducible induction of specific immune responses. Vaccine 2000; 18: 1725-1729.
25. Wang S, Zhang C, Zhang L, Li J, Huang Z, Lu S. The relative immunogenicity of DNA vaccines delivered by the intramuscular needle injection, electroporation and gene gun methods. Vaccine 2008; 26: 2100-2110.

Biochemical and Biophysical Research Communications 402 (2010) 790–795

Contents lists available at ScienceDirect

Biochemical and Biophysical Research Communications

journal homepage: www.elsevier.com/locate/ybbrc

Development of experimental cerebral malaria is independent of IL-23 and IL-17

Hidekazu Ishida [a,b], Chikako Matsuzaki-Moriya [a], Takashi Imai [b], Kunio Yanagisawa [b], Yoshihisa Nojima [c], Kazutomo Suzue [b], Makoto Hirai [b], Yoichiro Iwakura [d], Akihiko Yoshimura [e], Shinjiro Hamano [f], Chikako Shimokawa [f], Hajime Hisaeda [b,*]

[a] Department of Microbiology and Immunology, Graduate School of Medical Sciences, Kyushu University, Fukuoka 812-8582, Japan
[b] Department of Parasitology, Gunma University, Graduate School of Medicine, Gunma 371-8511, Japan
[c] Department of Medicine and Clinical Science, Gunma University, Graduate School of Medicine, Gunma 371-8511, Japan
[d] Center for Experimental Medicine, Institute of Medical Science, The University of Tokyo, Tokyo 108-8639, Japan
[e] Department of Microbiology and Immunology, School of Medicine, Keio University, Tokyo 160-8582, Japan
[f] Department of Parasitology, Institute of Tropical Medicine, Nagasaki University, Nagasaki 852-8523, Japan

ARTICLE INFO

Article history:
Received 21 October 2010
Available online 29 October 2010

Keywords:
Cerebral malaria
IL-23
IL-17
Immune responses
Malaria

ABSTRACT

Cerebral malaria (CM) is the most severe complication of *Plasmodium* infection. Although inappropriate immune responses to *Plasmodium falciparum* are reported as the major causes of CM, the precise mechanisms for development remain unclear. IL-23 and IL-17 have critical roles in the onset of autoimmunity and inflammatory diseases triggered by microbial infections. Thus, we investigated the influence of IL-23 and IL-17 on experimental CM (ECM) using *Plasmodium berghei* ANKA infection of C57BL/6 mice. Both IL-23 deficient mice and wild-type (WT) mice developed ECM. IL-17 deficient mice also developed ECM, while IL-17 producing cells other than $CD4^+$ T cells (Th17) were increased in WT mice that developed ECM. In conclusion, this study showed that IL-23 and IL-17 are not involved in ECM development.

1. Introduction

Malaria is a major life-threatening parasitic disease. Each year, 500 million cases and 2 million deaths are reported and 40% of the world's population is at risk of malaria infection [1]. Cerebral malaria (CM) associated with *Plasmodium falciparum* infection is responsible for almost all malaria deaths and is characterized by impaired consciousness/coma and generalized convulsions [2,3]. Approximately 1% of *P. falciparum* infected patients develop CM. The majority of these cases occur in young children in sub-Saharan Africa, of which, 10–20% are fatal and the remaining survivors acquire permanent neurological damage [4,5]. Histologically, multifocal capillary obstruction with parasitized red blood cells (RBC) and leukocytes is observed in brain tissue from patients that die of CM [6] and suggests *P. falciparum* infection may trigger vascular and immune system dysfunction. However, the precise mechanisms causing CM are not fully understood.

After the discovery of $CD4^+$ T cells producing IL-17 (Th17), a new subset of effector T helper cells, the immune responses involving IL-23 and IL-17 have been investigated in detail. IL-23 is a heterodimeric cytokine comprised of a p40 subunit and a unique p19 subunit [7]. Recently, it was revealed that IL-23 is critical for the development of Th17 [8] and for immune cell activation [9,10]. IL-17 is a proinflammatory cytokine secreted by immune cells and mediates granulopoiesis, infiltration of neutrophils and recruitment of T cells into peripheral tissues via the induction of chemokine and cytokine expression [11,12].

Many studies using *IL-23 p19*$^{-/-}$ mice (P19KO) and *IL-17*$^{-/-}$ mice (17KO) suggest that IL-23 and IL-17 play a critical role in the onset of autoimmune diseases, such as experimental autoimmune encephalitis, collagen induced arthritis and inflammatory bowel diseases [7,13–15]. Furthermore, as both cytokines contribute to the development of arthritis caused by *Borrelia burgdorferi* infection [16] and brain damage caused by *Toxoplasma gondii* infection [17], IL-23 and IL-17 may be associated with the immunopathology triggered by microorganism infection.

Infection of susceptible mouse strains with *Plasmodium berghei* ANKA (PbA) allows for the development of experimental CM (ECM) that shares some characteristics with CM. Immune cells, including T cells, antigen-presenting cells (APC), NK cells and neutrophils, play critical roles in the development of ECM [18–21]. During infection, these cells activate and cooperate with each other to allow T cell migration into brain. This results in blood–brain barrier (BBB) disruption and is a key pathological feature of ECM. IL-23 is

Abbreviations: IL-23, Interleukin-23; IL-17, Interleukin-17; RBC, red blood cell; Th, T helper cells; NK cells, natural killer cells; Treg, regulatory T cell.

* Corresponding author. Address: Department of Parasitology, Gunma University, Graduate School of Medicine, 3-39-22, Showa-machi, Maebashi, Gunma 371-8511, Japan. Fax: +81 27 220 8025.
E-mail address: hisa@med.gunma-u.ac.jp (H. Hisaeda).

0006-291X/$ - see front matter © 2010 Elsevier Inc. All rights reserved.
doi:10.1016/j.bbrc.2010.10.114

strongly associated with activation of APC and NK cells and also with development of Th17 that is capable BBB disruption [8–10]. IL-17 is involved in the activation and recruitment of neutrophils [11] and upregulation of CXCL 9, 10, and 11, which are ligands of CXCR3 essential for the migration of $CD8^+$ T cells into brain [12,22]. Given these findings, it is possible that IL-23 and/or IL-17 may contribute to development of ECM.

We therefore examined the role of IL-23 and IL-17 in ECM development using P19KO and 17KO mice. Our results demonstrated that P19KO mice developed ECM similarly to wild-type (WT) mice. 17KO mice also developed ECM while IL-17-producing cells other than $CD4^+$ T cells increased in WT mice during ECM. Thus, our results conclude that IL-23 and IL-17 may not be involved in ECM development.

2. Materials and methods

2.1. Mice and parasites

C57BL/6 mice were purchased from Kyudo (Tosu, Japan). Age and sex-matched groups of WT mice, P19KO mice and 17KO mice were used for experiments. All experiments that involved mice were reviewed by the Committee for Ethics on Animal Experiments in the Faculty of Medicine and were conducted under the control of the Guidelines for Animal Experiments in the Faculty of Medicine, Kyushu University and the Law (No. 105) and Notification (No. 6) of the Government. Blood-stage parasites of *P. berghei* ANKA (PbA) were a generous gift from Dr. M. Torii (Ehime University), obtained after fresh passage through a donor mouse, 2–3 days after inoculation with frozen stock. Mice were infected with 50,000 parasitized RBC (pRBC) via intraperitoneal injection.

2.2. Determination of parasitemia

Blood samples were collected from the tail vein of experimental mice at the time indicated. Thin blood films were prepared and fixed with methanol before being stained with Giemsa solution (Sigma–Aldrich, St. Louis, MO, USA). Parasitemia was determined by counting the percentage of infected RBC (pRBC) using light microscopy.

2.3. Preparation of brain-sequestered leukocytes (BSL) and spleen cells

BSL were prepared according to the previously described methods [23,24]. Briefly, sacrificed mice were intracardially perfused with PBS to remove both circulating, nonadherent RBC and leukocytes from the brain. The brain was then removed and crushed in RPMI1640 supplemented with 100 IU/mL penicillin, 100 mg/mL streptomycin, 20 mM HEPES, 2 mM L-glutamine, 100 mM 2-mercaptoethanol and 10% inactivated fetal bovine serum (complete medium). The tissue suspension was centrifuged at 400 *g* for 5 min and the pellet was resuspended with HEPES buffer, supplemented with 0.05% collagenase (Roche Applied Science, Indianapolis, IN, USA) and 2 U of DNase (Sigma–Aldrich, St. Louis, MO, USA)/ml. The mixture was stirred at room temperature for 60 min, then passed through a sterile gauze and centrifuged at 80 *g* for 30 s to remove debris. The supernatant was deposited on a 30% Percoll (Sigma–Aldrich, St. Louis, MO, USA) to remove brain cells and centrifuged at 1400 *g* for 10 min. The pellet was resuspended with medium to form single-cell suspensions. Residual RBC in single-cell suspensions prepared from the brain and spleen were lysed with NH_4Cl. Cells were then washed twice with fresh medium before being used for experiments. $CD4^+$ cells were purified with positive selection using a MACS cell separation system (Miltenyi Biotech) according to the manufacturer's protocols. Separated cell purity was generally >95%.

2.4. Real-time RT-PCR

Total RNA was extracted from BSL, spleen cells and $CD4^+$ cells before being reverse-transcribed to cDNA. mRNA that encoded genes of interest was quantified from cDNA by evaluating SYBR Green dye incorporation (Takara, Tokyo, Japan) using a real-time PCR system GeneAmp7000 thermal cycler (Applied Biosystems, Foster City, CA, USA). PCR was performed according to the manufacturer's protocols. Expression levels of target genes were determined as the difference of Ct between the β-actin-encoding gene and target gene using the following formula: $\Delta Ct = Ct_{\text{target gene}} - Ct_{\text{reference gene}}$. PCR primers used were as follows: for IL-23p19, 5′-TGGCTGTG CCTAGGAGTAGCA-3′ and 5′-TTCATCCTCTTCTTCTCTTAGTAGATTC ATA-3′; for IL-17, 5′-TCATCTGTGTCTCTGATGCTGTTG-3′ and 5′-TCG CTGCCTTCACTGT-3′; for RORγt, 5′-AGCAGTGTAATGTGGCCTAC-3′ and 5′- GCACTTCTGCATGTAGACTG-3′; and for β-actin, 5′-TGGAAT CCTGTGGCATCCATGAAAC-3′ and 5′-TAAAACGCAGCTCAGTAACAG TCCG-3′.

2.5. Flow cytometry

BSL and spleen cells were stained with a combination of fluorochrome-labeled antibodies. For intracellular staining, cells were stimulated with 50 ng/ml PMA and 500 ng/ml calcium ionophore in the presence of Golgi plug (BD Bioscience, San Jose, CA, USA), in complete medium at 37 °C for 4 h. Cells were then incubated with anti-CD16/32 (Fc-block) and stained with FITC-anti-CD4 (eBioscience, San Diego, CA, USA) followed by fixation/permeabilization with BD cytofix/cytoperm (BD Bioscience, San Jose, CA, USA) according to manufacturer's protocols. Cells were stained with PE-anti-IL-17 or PE-anti-IFN-γ (BD Bioscience, San Jose, CA, USA) and analyzed using a FACS Caliber cytometer (Becton Dickinson, San Jose, CA, USA). Data were analyzed using CellQuest Pro software (Becton Dickinson).

2.6. Histology

For histological analysis of cerebral pathology, brains from mice developing ECM were perfused with PBS and carefully removed and fixed in formaldehyde solution (4 v/v%). The 5-μm tissue sections were prepared and stained with hematoxylin and eosin (HE).

2.7. Statistical analysis

Statistical differences between experimental groups were evaluated using a two-tailed unpaired Student's *t*-test. Survival analysis was determined using Kaplan Meier survival analysis. $P < 0.05$ was considered statistically significant.

3. Results and discussion

3.1. IL-23 is not involved in the onset of ECM

C57BL/6 mice infected with PbA developed ECM that was characterized by neurological manifestations, such as ataxia, paralysis (monoplegia, hemiplegia and tetraplegia) and coma as early as 7 or 8 days after infection, and death occurred between 7 and 10 days after infection [25]. We first investigated the expression of IL-23 during ECM to assess the involvement of IL-23. BSL and spleen cells were collected and p19 mRNA expression was analyzed by quantitative RT-PCR. No significant difference in the expression of p19 mRNA was observed between mice developing ECM and uninfected control mice (Fig. 1A and B). Thus, PbA infection of mice did not induce IL-23 in both tissues sampled. Furthermore, to directly investigate the contribution of IL-23 to the

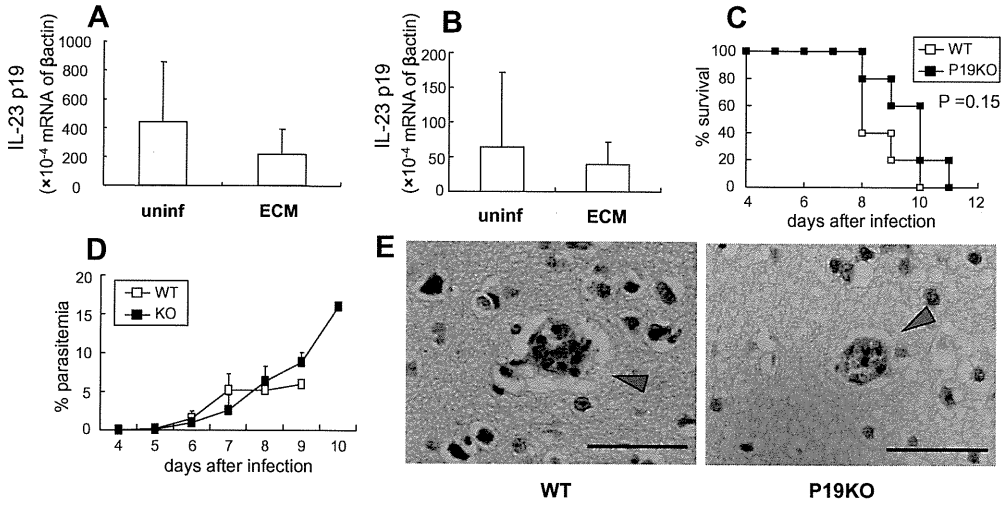

Fig. 1. ECM induced by PbA infection was independent of IL-23. mRNA encoding IL-23p19 in BSL (A) and spleen cells (B) isolated from mice developing ECM was quantified using RT-PCR. Values are relative to amounts of mRNA encoding β-actin. Data represent the mean ± SD of four mice. Survival rates (C) or parasitemia (D) of WT and P19KO mice infected with 50,000 PbA-pRBC were monitored. Each group is comprised of five mice. One representative of at least two repeated experiments is shown. Brains from WT (left panel) and P19KO mice (right panel) developing ECM were analyzed for histological examination (E). Representative histological sections from areas around the blood vessels of cerebrum with HE staining are shown (original magnification, ×1000). Arrowheads indicate accumulation of mononuclear cells and erythrocytes. Scale bars equal 50 μm.

development of ECM, P19KO mice were infected with PbA. Infected P19KO as well as WT mice showed severe neurological symptoms and died within 11 days when the parasitemia was lower than 10% (Fig. 1C, D), suggesting that P19KO mice developed ECM. To confirm development of ECM in these mutants, histological analyses of brains isolated from P19KO mice developing ECM were performed. Both P19KO and WT mice showed cerebral blood vessels sequestered with mononuclear cells and erythrocytes, a typical sing of ECM induced by PbA (Fig. 1E). No sequestered vessel was observed before infection (data not shown). These results clearly demonstrated that the development of ECM does not require IL-23.

3.2. IL-17 does not contribute to ECM development

To assess whether IL-17 contributes to ECM, we analyzed IL-17 producing cells using flow cytometry. IL-17 producing cells were increased in the brain and spleen of mice developing CM when compared to uninfected control mice (Fig. 2A and C). The emergence of Th17 during ECM was also investigated as an assessment of IL-17 production. Mice that developed ECM showed a higher frequency and absolute number of $CD4^+$ IFN-γ^+ Th1 cells (IFN-γ^+ $CD4^+$ cells (Th1)) in the brain and spleen when compared to uninfected control mice (Fig. 2B and C), which supported previous study [26]. By contrast, there were no differences in the frequency and absolute number of Th17 between mice that developed ECM and uninfected control mice (Fig. 2A and C). Furthermore, we analyzed the expression of mRNAs encoding IL-17 and a "master-regulator" transcription factor of Th17, RORγt, in $CD4^+$ cells purified from BSL and spleen cells. Mice that developed ECM showed lower mRNA expression levels compared to uninfected mice (Fig. 3A and B). These results demonstrate that IL-17-producing cells other than Th17 developed during ECM. Finally, to directly investigate the contribution of IL-17 to onset of ECM, 17KO mice were infected with PbA. Both infected 17KO mice and infected WT mice developed neurological symptoms and died (Fig. 4A) and produced no differences in parasitemia kinetics (Fig. 4B). Histological examination of brain sections revealed that 17KO as well as WT mice showed leukocyte-packed vessels (Fig. 4C). These results demonstrate that the development of ECM is independent of IL-17.

3.3. General discussion

As observed during our study, infection with PbA did not induce the expression of IL-23 and a lack of IL-23 did not affect the develop ECM. Moreover, IL-17 deficient mice also develop ECM, while IL-17 producing cells increased in WT mice affected with ECM. These results suggest that both cytokines are unnecessary for the development of ECM.

Th17 development was not observed during infection with PbA primarily because IL-23, which is critical for Th17 expansion, was not secreted. We confirmed that expression of mRNA encoding IL-17 or RORγt in $CD4^+$ T cells decreased in mice that developed ECM and that the frequency and cell number of Th17 were not increased. In addition, environments under malaria infection favor to induce Treg [29,30], consequently might disturb Th17 differentiation as a counter-regulatory action [31]. By contrast, we observed that the frequency of Th1 was increased in WT mice that developed ECM (Supplementary Fig. 1). Expression of mRNA encoding T-bet or IFN-γ in $CD4^+$ T cells from mice that developed ECM were higher than those from uninfected mice (data not shown). These findings suggested that Th1 rather than Th17 may be of importance in ECM development and supports previous suggestions that Th1 are dominant during ECM [26].

IL-17 is known to suppress pathogenic Th1 responses during inflammatory bowel disease [27,28], suggesting that augmented induction of Th1 covers or compensates lack of IL-17-mediated pathogenesis in ECM development. However, there was no difference between WT and 17KO mice in Th1 induced by infection with PbA (Supplementary Fig. 1). Given these results, it appears that IL-17 does not suppress Th1 responses during ECM and thus does not contribute to ECM development.

In addition to the ECM produced by PbA infection, hepatic injury observed in mice infected with *P. berghei* NK65 (PbNK) is also reported to be immunopathological [1,32]. Our preliminary results revealed that P19KO mice or 17KO mice infected with PbNK displayed elevated serum levels of enzymes released from the damaged hepatocytes, as was the case for WT mice (data not shown). Thus, these cytokines do not appear to be involved in ECM development or liver injury by infection with PbNK. Immunopathologies

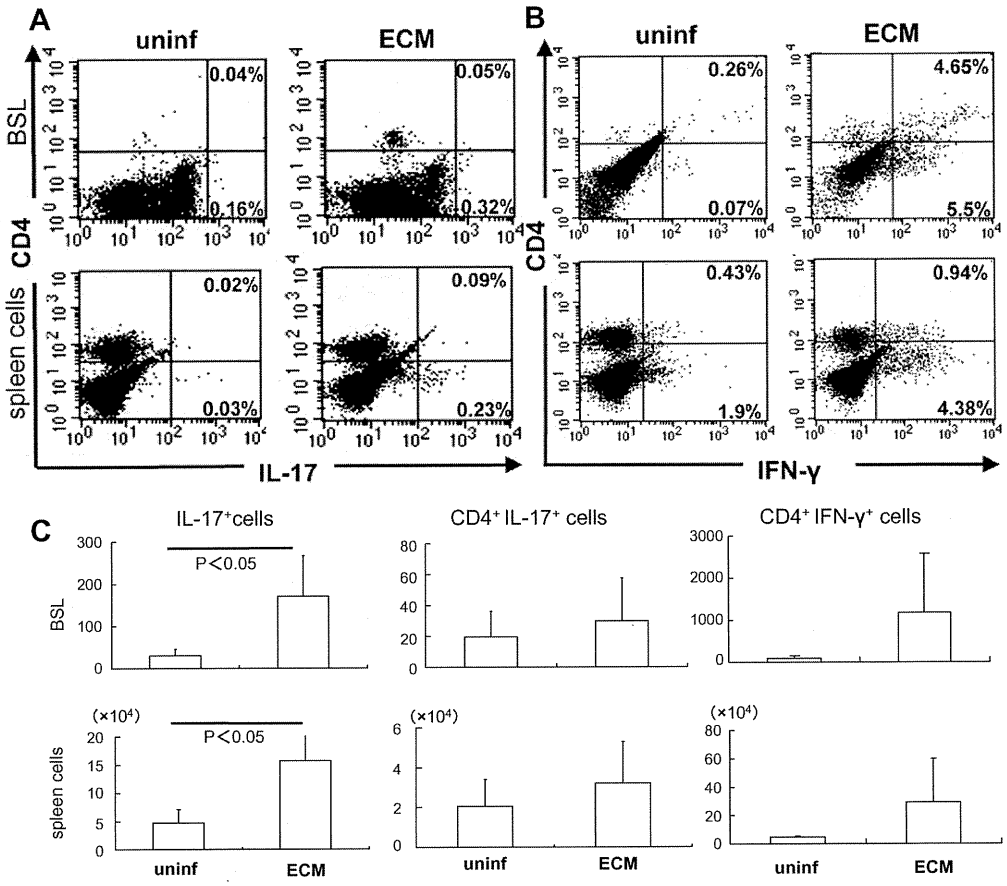

Fig. 2. Induction of IL-17-producing cells during infection with PbA. BSL (upper panel) or spleen cells (lower panel) isolated from mice that developed ECM were analyzed for IL-17 (A) and IFN-γ (B) production. Gated lymphocytes were plotted for CD4 and each cytokine. The numbers indicate the percentage of quadrants. Absolute numbers of the indicated cells were also shown (C). Data represent the mean ± SD of five mice. One representative of at least two repeated experiments is shown.

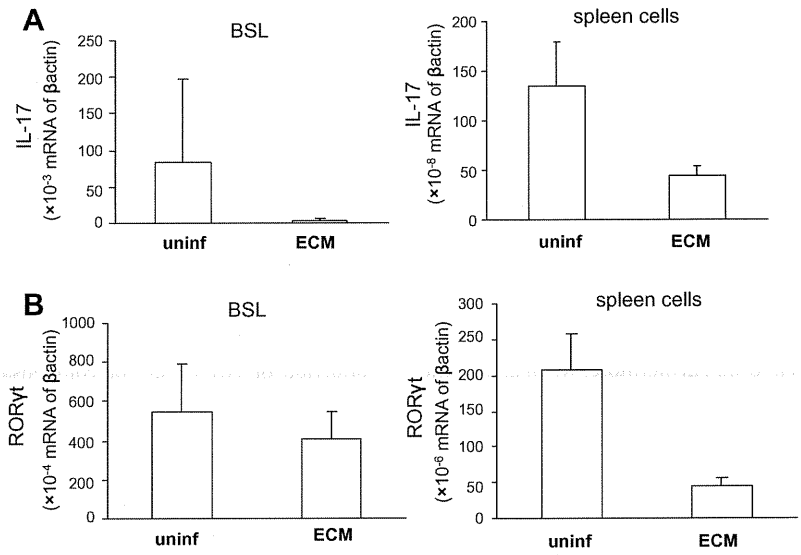

Fig. 3. Induction of Th17 in mice infected with PbA. CD4⁺ cells were purified from BSL and spleen cells of mice developing ECM and analyzed for the expression of mRNA encoding IL-17 (A) and RORγt (B) as in Fig. 1A. One representative of at least two repeated experiments is shown.

induced by malaria parasites may therefore be independent of IL-23 and IL-17, unlike other infectious diseases.

IL-23 and IL-17 are reported to be protective against some infections [33], yet are responsible for inflammatory pathologies

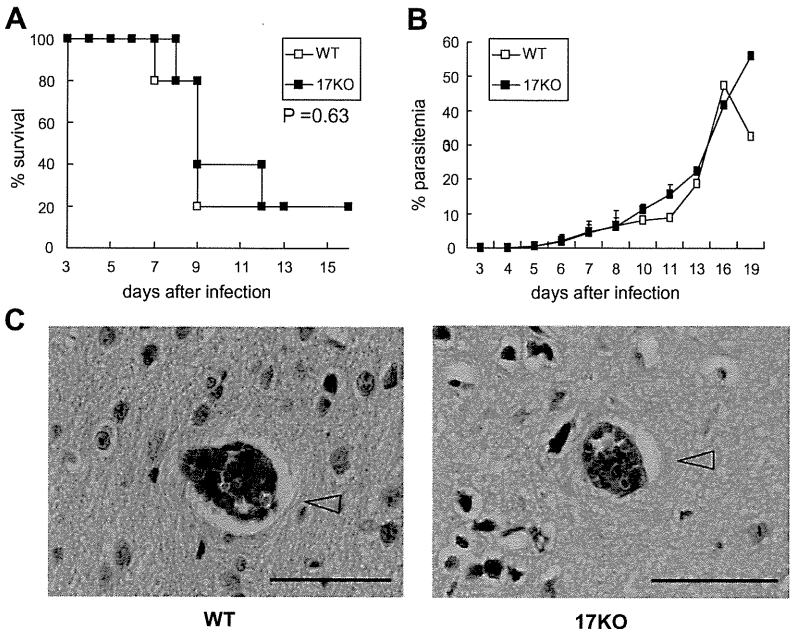

Fig. 4. ECM induced by PbA infection was independent of IL-17. Survival rates (A) or parasitemia (B) of WT and 17KO mice infected with 50,000 PbA-pRBC were monitored as in Fig. 1C. Histological analysis of brain sections of WT (left panels) and 17KO mice (right panels) developing ECM was performed as in Fig. 1E.

in other situations. Parasitemia in P19KO or 17KO mice infected with PbA was similar to that in infected WT mice. These findings suggest that IL-23 and IL-17 do not contribute to the reduction of parasite burdens in mice infected with PbA. However, those cytokines have protective effects against infection with PbNK65 and the lack of IL-23 shortened the survival of infected mice. IL-23 also has anti-protozoan effects against *Plasmodium yoelii* XL (manuscript in preparation). The protective effects of IL-23 and IL-17 during malaria therefore appear to dependent on the species and strain of malaria parasites.

In conclusion, IL-23 and IL-17 are not critical for the development of ECM, a complicated pathology that is produced in association with various immune cells, cytokines and chemokines. It would also be of interest to investigate whether similar results could be achieved using human patients. Such insights will potentially further our understanding CM pathogenesis and help establish new therapeutic strategies.

Acknowledgments

The authors thank Rumiko Koitabashi for handling and support with brain sections. This work was supported by grants from the Ministry of Education, Science Sport and Culture of Japan to H.H. (20390121, 21022036).

Appendix A. Supplementary data

Supplementary data associated with this article can be found, in the online version, at doi:10.1016/j.bbrc.2010.10.114.

References

[1] M.F. Good, H. Xu, M. Wykes, C.R. Engwerda, Development and regulation of cell-mediated immune responses to the blood stages of malaria: implications for vaccine research, Annu. Rev. Immunol. 23 (2005) 69–99.
[2] G.G. MacPherson, M.J. Warrell, N.J. White, S. Looareesuwan, D.A. Warrell, Human cerebral malaria. A quantitative ultrastructural analysis of parasitized erythrocyte sequestration, Am. J. Pathol. 119 (1985) 385–401.
[3] L.H. Miller, D.I. Baruch, K. Marsh, O.K. Doumbo, The pathogenic basis of malaria, Nature 415 (2002) 673–679.
[4] Roll Back Malaria: spotlight on Africa, TDR News (2000) 10, 15.
[5] R.W. Snow, J.F. Trape, K. Marsh, The past, present and future of childhood malaria mortality in Africa, Trends Parasitol. 17 (2001) 593–597.
[6] H.C. van der Heyde, J. Nolan, V. Combes, I. Gramaglia, G.E. Grau, A unified hypothesis for the genesis of cerebral malaria: sequestration, inflammation and hemostasis leading to microcirculatory dysfunction, Trends Parasitol. 22 (2006) 503–508.
[7] R.A. Kastelein, C.A. Hunter, D.J. Cua, Discovery and biology of IL-23 and IL-27: related but functionally distinct regulators of inflammation, Annu. Rev. Immunol. 25 (2007) 221–242.
[8] E. Bettelli, T. Korn, M. Oukka, V.K. Kuchroo, Induction and effector functions of T(H)17 cells, Nature 453 (2008) 1051–1057.
[9] C.L. Langrish, B.S. McKenzie, N.J. Wilson, R. de Waal Malefyt, R.A. Kastelein, D.J. Cua, IL-12 and IL-23: master regulators of innate and adaptive immunity, Immunol. Rev. 202 (2004) 96–105.
[10] W. Sun, X. He, Z. Guo, Q. Wang, X. Li, J. Rayner, L. Zhang, J. Wang, X. Cao, IL-12p40-overexpressing immature dendritic cells induce T cell hyporesponsiveness in vitro but accelerate allograft rejection in vivo: role of NK cell activation and interferon-gamma production, Immunol. Lett. 94 (2004) 191–199.
[11] C.T. Weaver, R.D. Hatton, P.R. Mangan, L.E. Harrington, IL-17 family cytokines and the expanding diversity of effector T cell lineages, Annu. Rev. Immunol. 25 (2007) 821–852.
[12] S.A. Khader, G.K. Bell, J.E. Pearl, J.J. Fountain, J. Rangel-Moreno, G.E. Cilley, F. Shen, S.M. Eaton, S.L. Gaffen, S.L. Swain, R.M. Locksley, L. Haynes, T.D. Randall, A.M. Cooper, IL-23 and IL-17 in the establishment of protective pulmonary $CD4^+$ T cell responses after vaccination and during mycobacterium tuberculosis challenge, Nat. Immunol. 8 (2007) 369–377.
[13] W. Ouyang, J.K. Kolls, Y. Zheng, The biological functions of T helper 17 cell effector cytokines in inflammation, Immunity 28 (2008) 454–467.
[14] E. Bettelli, M. Oukka, V.K. Kuchroo, T(H)-17 cells in the circle of immunity and autoimmunity, Nat. Immunol. 8 (2007) 345–350.
[15] C.M. Tato, D.J. Cua, Reconciling id, ego, and superego within interleukin-23, Immunol. Rev. 226 (2008) 103–111.
[16] J. Knauer, S. Siegemund, U. Muller, S. Al-Robaiy, R.A. Kastelein, G. Alber, R.K. Straubinger, Borrelia burgdorferi potently activates bone marrow-derived conventional dendritic cells for production of IL-23 required for IL-17 release by T cells, FEMS Immunol. Med. Microbiol. 49 (2007) 353–363.
[17] J.S. Stumhofer, A. Laurence, E.H. Wilson, E. Huang, C.M. Tato, L.M. Johnson, A.V. Villarino, Q. Huang, A. Yoshimura, D. Sehy, C.J. Saris, J.J. O'Shea, L. Hennighausen, M. Ernst, C.A. Hunter, Interleukin 27 negatively regulates the development of interleukin 17-producing T helper cells during chronic inflammation of the central nervous system, Nat. Immunol. 7 (2006) 937–945.
[18] D.S. Hansen, N.J. Bernard, C.Q. Nie, L. Schofield, NK cells stimulate recruitment of $CXCR3^+$ T cells to the brain during *Plasmodium berghei*-mediated cerebral malaria, J. Immunol. 178 (2007) 5779–5788.

[19] C. Engwerda, E. Belnoue, A.C. Gruner, L. Renia, Experimental models of cerebral malaria, Curr. Top. Microbiol. Immunol. 297 (2005) 103–143.
[20] L. Chen, Z. Zhang, F. Sendo, Neutrophils play a critical role in the pathogenesis of experimental cerebral malaria, Clin. Exp. Immunol. 120 (2000) 125–133.
[21] S. deWalick, F.H. Amante, K.A. McSweeney, L.M. Randall, A.C. Stanley, A. Haque, R.D. Kuns, K.P. MacDonald, G.R. Hill, C.R. Engwerda, Cutting edge: conventional dendritic cells are the critical APC required for the induction of experimental cerebral malaria, J. Immunol. 178 (2007) 6033–6037.
[22] J. Miu, A.J. Mitchell, M. Muller, S.L. Carter, P.M. Manders, J.A. McQuillan, B.M. Saunders, H.J. Ball, B. Lu, I.L. Campbell, N.H. Hunt, Chemokine gene expression during fatal murine cerebral malaria and protection due to CXCR3 deficiency, J. Immunol. 180 (2008) 1217–1230.
[23] E. Belnoue, M. Kayibanda, A.M. Vigario, J.C. Deschemin, N. van Rooijen, M. Viguier, G. Snounou, L. Renia, On the pathogenic role of brain-sequestered alphabeta CD8$^+$ T cells in experimental cerebral malaria, J. Immunol. 169 (2002) 6369–6375.
[24] T. Voza, A.M. Vigario, E. Belnoue, A.C. Gruner, J.C. Deschemin, M. Kayibanda, F. Delmas, C.J. Janse, B. Franke-Fayard, A.P. Waters, I. Landau, G. Snounou, L. Renia, Species-specific inhibition of cerebral malaria in mice coinfected with *Plasmodium* spp., Infect. Immun. 73 (2005) 4777–4786.
[25] J. Hearn, N. Rayment, D.N. Landon, D.R. Katz, J.B. de Souza, Immunopathology of cerebral malaria: morphological evidence of parasite sequestration in murine brain microvasculature, Infect. Immun. 68 (2000) 5364–5376.
[26] N.H. Hunt, G.E. Grau, Cytokines: accelerators and brakes in the pathogenesis of cerebral malaria, Trends Immunol. 24 (2003) 491–499.
[27] C.L. Maynard, C.T. Weaver, Intestinal effector T cells in health and disease, Immunity 31 (2009) 389–400.
[28] W. O'Connor Jr., M. Kamanaka, C.J. Booth, T. Town, S. Nakae, Y. Iwakura, J.K. Kolls, R.A. Flavell, A protective function for interleukin 17A in T cell-mediated intestinal inflammation, Nat. Immunol. 10 (2009) 603–609.
[29] H. Hisaeda, Y. Maekawa, D. Iwakawa, H. Okada, K. Himeno, K. Kishihara, S. Tsukumo, K. Yasutomo, Escape of malaria parasites from host immunity requires CD4$^+$ CD25$^+$ regulatory T cells, Nat. Med. 10 (2004) 29–30.
[30] T.T. Long, S. Nakazawa, S. Onizuka, M.C. Huaman, H. Kanbara, Influence of CD4$^+$ CD25$^+$ T cells on *Plasmodium berghei* NK65 infection in BALB/c mice, Int. J. Parasitol. 33 (2003) 175–183.
[31] E. Bettelli, Y. Carrier, W. Gao, T. Korn, T.B. Strom, M. Oukka, H.L. Weiner, V.K. Kuchroo, Reciprocal developmental pathways for the generation of pathogenic effector TH17 and regulatory T cells, Nature 441 (2006) 235–238.
[32] A. Bhalla, V. Suri, V. Singh, Malarial hepatopathy, J. Postgrad. Med. 52 (2006) 315–320.
[33] F.L. van de Veerdonk, M.S. Gresnigt, B.J. Kullberg, J.W. van der Meer, L.A. Joosten, M.G. Netea, Th17 responses and host defense against microorganisms: an overview, BMB Rep. 42 (2009) 776–787.

INFECTION AND IMMUNITY, Oct. 2011, p. 3947–3956 Vol. 79, No. 10
0019-9567/11/$12.00 doi:10.1128/IAI.01337-10

Prevention of Experimental Cerebral Malaria by Flt3 Ligand during Infection with *Plasmodium berghei* ANKA▽†

Takahiko Tamura,[1,2] Kazumi Kimura,[1] Masao Yuda,[3] and Katsuyuki Yui[1,2]*

Division of Immunology, Department of Molecular Microbiology and Immunology, Graduate School of Biomedical Sciences,[1] and Global COE Program,[2] Nagasaki University, 1-12-4 Sakamoto, Nagasaki 852-8523, and Department of Medical Zoology, School of Medicine, Mie University, 2-174 Ed. bashi Tsu, Mie 514-8507,[3] Japan

Received 19 December 2010/Returned for modification 24 January 2011/Accepted 20 July 2011

Dendritic cells are the most potent antigen-presenting cells, but their roles in blood-stage malaria infection are not fully understood. We examined the effects of Flt3 ligand, a cytokine that induces dendritic cell production, *in vivo* on the course of infection with *Plasmodium berghei* ANKA. Mice treated with Flt3 ligand showed preferential expansion of CD8$^+$ dendritic cells and granulocytes, as well as lower levels of parasitemia, and were protected from the development of lethal experimental cerebral malaria (ECM). Rag2 knockout mice treated with Flt3 ligand also showed inhibition of parasitemia, suggesting that this protection was due, at least in part, to the stimulation of innate immunity. However, it was unlikely that the inhibition of ECM was due simply to the reduction in the level of parasitemia. In the peripheral T cell compartment, CD8$^+$ T cell levels were markedly increased in Flt3 ligand-treated mice after infection. These CD8$^+$ T cells expressed CD11c and upregulated CXCR3, while the expression of CD137, CD25, and granzyme B was reduced. In the brain, the number of sequestered CD8$^+$ T cells was not significantly different for treated versus untreated mice, while the proportion of CD8$^+$ T cells that produce gamma interferon (IFN-γ) and granzyme B was significantly reduced in treated mice. In addition, sequestration of parasitized red blood cells (RBCs) in the brain was reduced, suggesting that altered CD8$^+$ T cell activation and reduced sequestration of parasitized RBCs culminated in inhibition of ECM development. These results suggest that the quantitative and qualitative changes in the dendritic cell compartment are important for the pathogenesis of ECM.

Malaria is one of the most serious infections in the world and is responsible for more than 1 million deaths each year. Infection with *Plasmodium falciparum* induces a wide range of severe pathologies, including cerebral malaria (CM), one of the major causes of mortality due to this important parasite (14, 29, 36). Infection with *Plasmodium berghei* ANKA, a rodent malaria parasite, induces neurological symptoms and death in C57BL/6 (B6) and CBA mice and is widely used as a mouse model of experimental cerebral malaria (ECM) (9). Previous studies using the *P. berghei* ANKA infection model indicate the importance of brain-sequestered CD8$^+$ T cells in the pathogenesis of ECM. Depletion of CD8$^+$ T cells in C57BL/6 mice prevented the development of ECM, while reconstitution of CD8$^+$ T cells in recombination-activating gene (RAG)-deficient mice, which lack both T and B cells, resulted in the development of ECM after infection with *P. berghei* ANKA (3, 26). In addition, concomitant accumulation of parasitized red blood cells (pRBC) in the brain is critical for the development of ECM (1). The recruitment of CD8$^+$ T cells to the brain and the pathogenesis of ECM are dependent on chemokine receptor CCR5 (2, 26) and on CXCR3 expressed on CD8$^+$ T cells, as well as on the CXCR3 ligands CXCL9/CXCL10 (6, 24, 37). In the effector phase, the production of proinflammatory cytokines, such as gamma interferon (IFN-γ), and the cytotoxic activity of CD8$^+$ T cells play critical roles in the pathogenesis of ECM (26, 40).

CD11c$^+$ dendritic cells (DCs) are professional antigen-presenting cells that can prime naïve T cells, leading to the development of effector T cells. DCs can phagocytose malaria-parasitized red blood cells during infection and can present malaria antigen in both the major histocompatibility complex (MHC) class I and class II pathways, activating malaria-specific CD8$^+$ and CD4$^+$ T cells, respectively, and thus playing critical roles in the induction of protective immunity against *Plasmodium* infection (15, 17, 19, 20, 25, 33). However, DCs also play an important role in the pathogenesis of ECM, a T cell-dependent disease. It has been shown previously that depletion of conventional DCs, but not plasmacytoid DCs, resulted in reduced activation of malaria-specific T cells and inhibition of ECM development (10). The regulatory function of DCs in the pathogenesis of CM, however, is not completely understood.

Flt3 ligand (Flt3L) is an important cytokine for the differentiation and homeostasis of DCs (32). DCs differentiate from Flt3$^+$ progenitor cells at steady state (16). Administration of Flt3L induces a drastic increase in the number of DCs in the spleen and lymph nodes (21). In contrast, the lack of Flt3L leads to severe reductions in DC numbers in many tissues (22). It has been shown previously that the number and phenotype of DCs in the spleen fluctuated during infection with malaria parasites (33, 39). However, it was not clear what effect this fluctuation of DC numbers had on the priming of malaria-specific T cells and the pathogenesis of ECM. In this study, we

* Corresponding author. Mailing address: Division of Immunology, Department of Molecular Microbiology and Immunology, Graduate School of Biomedical Sciences, 1-12-4 Sakamoto, Nagasaki 852-8523, Japan. Phone: 81-95-819-7070. Fax: 81-95-819-7073. E-mail: katsu@nagasaki-u.ac.jp.

† Supplemental material for this article may be found at http://iai.asm.org/.

▽ Published ahead of print on 1 August 2011.

stimulated the expansion of DCs *in vivo* by administration of Flt3L prior to infection with *P. berghei* ANKA and examined the effects of Flt3L on the activation of the immune system as well as on the development of ECM. The results showed that Flt3L-treated mice were protected from ECM and exhibited altered T cell activation phenotypes. These studies suggest an important regulatory function for DCs in the activation of T cells as well as in the pathogenesis of ECM.

MATERIALS AND METHODS

Mice and plasmid transduction. Rag-2$^{-/-}$ mice of the C57BL/6 background (31) were provided by Y. Yoshikai (Kyushu University, Fukuoka, Japan), and were maintained in the Laboratory Animal Center for Animal Research at Nagasaki University. C57BL/6 mice were purchased from SLC (Hamamatsu, Japan). The animal experiments reported here were conducted according to the guidelines of the Laboratory Animal Center for Biomedical Research at Nagasaki University.

The coding sequence for the extracellular domain (amino acids 1 to 189) of mouse Flt3L was obtained by PCR from cDNA prepared from mouse spleen using primer pairs 5′-GATCCACCATGACAGTGCTGGCGCCAGC-3′ and 5′-GATCTACTGCCTGGGCCGAGGCTCTG-3′. After confirmation of the sequence, the PCR product was cloned into pCAGGS, resulting in pCAGGS-Flt3L. The plasmid was purified using the PureYield Plasmid Maxiprep system (Promega, Madison, WI), and its endotoxin level was 2.43 endotoxin units (EU) (equivalent to 0.55 ng endotoxin) per μg DNA, as determined by a *Limulus* test (Wako, Osaka, Japan). A solution containing the plasmid (5 μg in phosphate-buffered saline [PBS]) was injected into mice using the hydrodynamics method, as previously described (12).

GFP-expressing parasites and *P. berghei* ANKA infection. *P. berghei* ANKA was originally obtained from R. E. Sinden (Imperial College London, London, United Kingdom). Recombinant *P. berghei* strain ANKA parasites that constitutively express green fluorescent protein (PbKA-GFP) were engineered as previously described (25). The gene construct, based on pBluescript KS(+) (Stratagene), contains a *P. berghei* ANKA dihydrofolate reductase-thymidylate synthase (DHFR-ts) gene, the *P. berghei* ANKA hsp70 5′ untranslated region, its N-terminal coding sequence, and the coding sequence of GFP. *P. berghei* ANKA merozoites were transfected with the DNA construct by electroporation and were selected in rats by using pyrimethamine. Surviving parasites were cloned by limiting dilution in mice.

P. berghei ANKA was maintained by passage through BALB/c mice. For infection, mice were inoculated intraperitoneally (i.p.) with parasitized red blood cells (pRBC) (1×10^6, except where otherwise indicated). Parasitemia of infected mice was monitored by microscopic examination of Giemsa-stained tail blood smears. Typically, 5 to 6 days after infection with *P. berghei* ANKA, mice began to show neurological signs, such as hunching, paralysis, and ataxia, and they succumbed to death within 10 days of infection (6). A PBS solution containing 2% Evans blue dye was injected into mice on day 6 after *P. berghei* ANKA infection. After 1 h, mice were euthanized, and their brains were removed, fixed in a 3% paraformaldehyde solution, and photographed.

Flow cytometry. For the preparation of DCs, spleens were cut into small fragments, incubated with RPMI 1640 containing collagenase (100 U/ml), mechanically disrupted, and filtered to prepare single-cell suspensions. After the lysis of RBC, cells were stained with fluorescein isothiocyanate (FITC)-conjugated anti-CD4 (FITC–anti-CD4), allophycocyanin (APC)–anti-CD8, FITC–anti-MHC class II, FITC–anti-CD40, FITC–anti-CD80, FITC–anti-CD86, phycoerythrin (PE)–anti-CD11c, PE-Cy7–anti-CD3ε, PE-Cy7–anti-CD19, PE-Cy7–anti-NK1.1, PE-Cy7–anti-Ter119, FITC–anti-T cell receptor beta (TCRβ), FITC–anti-F4/80, PE–anti-Gr1, APC–anti-Ly6G, APC–anti-CD45, APC-Cy7–anti-Ly6C, APC-Cy7–anti-CD45, biotin–anti-DX5, biotin–anti-CD11c, and biotin–anti-CD11b antibodies (Abs) and PE-Cy7- or APC-streptavidin. Antibodies were purchased from BD Biosciences (San Jose, CA), eBioscience (San Diego, CA), or BioLegend (San Diego, CA). For intracellular staining of IFN-γ and granzyme B, splenocytes or brain-sequestered leukocytes were cultured on plates coated with an anti-TCR monoclonal Ab (MAb) (H57; 2 μg/ml) for 5 h, with the addition of GolgiStop (BD Biosciences) during the final 4 h. The cells were collected and stained with an anti-IFN-γ or anti-granzyme B MAb according to the manufacturer's instructions. For intracellular staining of Foxp3, splenocytes were stained using an anti-Foxp3 staining set (eBioscience) according to the manufacturer's instructions. Cells were analyzed using a FACSCanto II flow cytometer (BD Biosciences), and data were analyzed using CellQuest software. The following cell populations were defined: DCs (CD11c^{high} CD3ε$^-$ CD19$^-$ DX5$^-$), NK cells (NK1.1$^+$ TCRβ$^-$), macrophages (F4/80^{high} CD11b^{low} CD11c$^-$), and granulocytes (Gr1^{high} Ly6G$^+$ CD11b$^+$).

Cytokine quantification. Serum IFN-γ and Flt3L levels were quantified using a cytometric bead array (CBA) assay (BD Biosciences) and a mouse Flt3 ligand Quantikine enzyme-linked immunosorbent assay (ELISA) kit (R&D Systems, Minneapolis, MN), respectively. Splenic CD4$^+$ and CD8$^+$ T cells were purified using an anti-CD4 or anti-CD8 IMag cell separation system (BD Biosciences), respectively. Splenic DCs were purified using anti-CD11c magnetic cell sorting (MACS) microbeads and an autoMACS separator (Miltenyi Biotec, Bergisch Gladbach, Germany) or by sorting of CD11c$^+$ MHC class II$^+$ cells using a FACSAria flow cytometer (BD Biosciences). CD4$^+$ or CD8$^+$ T cells (1×10^5/well) were cultured for 48 h on 96-well plates coated with an anti-TCR MAb (H57; 2 μg/ml) or with DCs (3×10^4/well) pulsed with an RBC lysate (1 mg/ml) for 2 h. The levels of IFN-γ in the supernatant were determined by ELISA as described previously (25).

Preparation of brain-sequestered leukocytes and RBC. Mice were sacrificed 6 days after *P. berghei* ANKA infection, and brain-sequestered leukocytes were prepared as previously described with slight modifications (24). Briefly, euthanized mice were perfused intracardially with PBS, and brains were removed. Brains were crushed and treated with collagenase (100 U/ml) at 37°C for 15 min. The brain extract was centrifuged at 1,500 rpm for 20 min in a 30% Percoll solution to remove debris, and the cell pellet was collected. Cells were treated with Gey's solution to remove RBC, stained with antibodies, and analyzed by flow cytometry. After gating for CD45$^+$ Ter119$^-$ cells, CD4$^+$ and CD8$^+$ T cells were defined as TCRβ$^+$ CD4$^+$ and TCRβ$^+$ CD8$^+$ cells, respectively. For analysis of pRBC, total numbers of RBC were counted after Percoll centrifugation of brain extracts without RBC lysis. Cells were stained with PE-Cy7–anti-Ter119 and APC–anti-CD45 MAbs and were analyzed using a FACSCanto II flow cytometer. The proportion of pRBC was determined by microscopic examination in a manner similar to that of standard blood films. The number of pRBC in the brain was calculated by multiplying the number of RBC by the proportion of pRBC.

Depletion of neutrophils. The hybridoma cell line secreting MAb RB6-8C5 (anti-Gr1) was provided by H. Asao (Yamagata University, Yamagata, Japan) (7). Cells were cultured using the CELLine system (BD Biosciences), and the supernatant was purified using a HiTrap protein G HP column (GE Healthcare). To deplete neutrophils, mice received an i.p. injection of the MAb (50 μg) 2 days before the infection. Anti-Gr1 MAb RB6-8C5 is specific for both Ly6C and Ly6G (11). Since Ly6C is expressed on some T cells, we used 50 μg MAb, which depleted >99% of Ly6G$^+$ granulocytes while maintaining the majority of T cells (>85%) 2 days after the treatment. Under the conditions used, we estimated that the effect on the Ly6C$^+$ population was minimal.

Statistics. Results are expressed as means ± standard deviations (SD). Statistical analysis was performed using the Mann-Whitney test for the comparison of two experimental groups or the log rank test for survival, and the data were calculated using GraphPad Prism software (version 4.0). Differences with a P value of <0.05 were considered significant.

RESULTS

Prevention of cerebral malaria by Flt3L treatment. We introduced a plasmid encoding mouse Flt3L into C57BL/6 mice by using the hydrodynamics method to stimulate the expansion of DCs *in vivo*. The serum Flt3L concentration was significantly increased 1 week after Flt3L treatment (Fig. 1A). The numbers of DCs and granulocytes in the spleens of treated mice were significantly increased as previously reported (38), while the numbers of NK cells and macrophages were not increased (Fig. 1B). The number of RBC in peripheral blood was also unchanged, consistent with the previous report that megakaryocyte/erythrocyte progenitors in the bone marrow do not express Flt3 and that their populations do not expand after Flt3L administration (16). We next examined DC subpopulations and their expression of MHC and costimulatory molecules (Fig. 1C). The proportion of CD8$^+$ DCs was increased, while that of CD4$^+$ DCs was reduced, in the spleens of Flt3L-treated mice compared with those in untreated mice. The

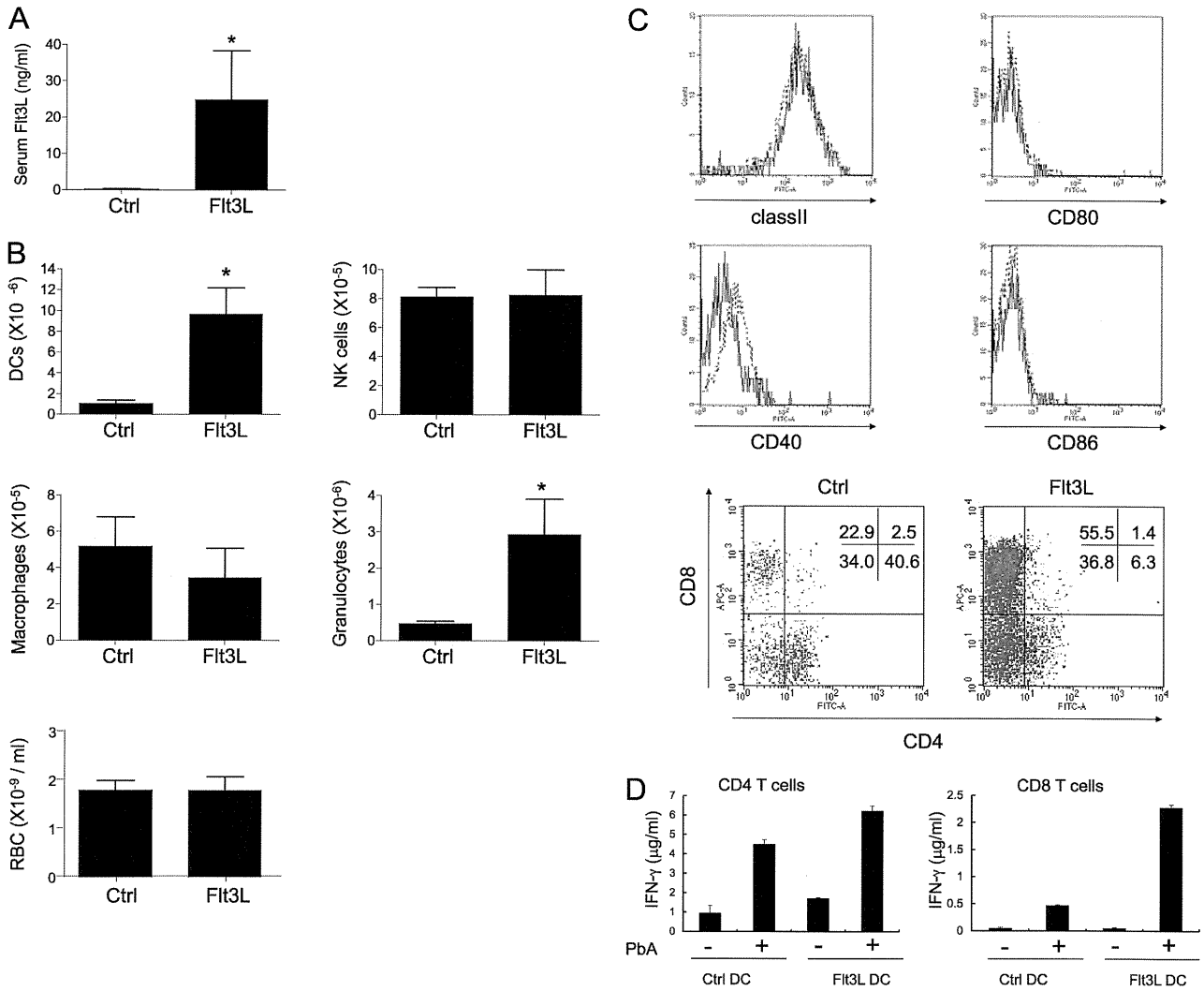

FIG. 1. Expansion of splenic DCs by expression of exogenous Flt3L. (A) Mice were inoculated (4 mice) or not (5 mice) with plasmid pCAGGS-Flt3L (5 μg) by the hydrodynamics method. After 7 days, serum was collected, and the level of Flt3L was determined by ELISA. Ctrl, control. (B) Splenocytes were stained with antibodies, and the numbers of DCs ($CD11c^{high}$ $CD3^-$ $CD19^-$ $DX5^-$), NK cells ($TCR\beta^-$ $NK1.1^+$), macrophages ($CD11c^-$ $F4/80^{high}$ $Gr1^-$), and granulocytes ($CD11c^-$ $Gr1^{high}$ $F4/80^-$) were determined by multiplying the total number of spleen cells by the ratio of each cell type. The number of RBC ($Ter119^+$ $CD45^-$) in peripheral blood was also determined. Asterisks indicate that a significant difference was observed between untreated and Flt3L-treated mice (P, < 0.05 by the Mann-Whitney test). (C) Splenocytes from mice that were either left untreated (solid lines) or treated with pCAGGS-Flt3L (dotted lines) were stained with antibodies, and flow cytometric analysis of MHC class II, CD80, CD86, CD40, and CD4 versus CD8 on DCs was conducted. (D) DCs (3×10^4) were prepared from untreated or Flt3L-treated mice, pulsed with or without pRBC lysates (1 mg/ml), and cocultured with splenic $CD4^+$ or $CD8^+$ T cells (1×10^5) from *P. berghei* ANKA-infected mice. After 48 h, the levels of IFN-γ in the supernatant were determined by ELISA. The experiments were repeated twice, and representative data are shown.

expression levels of MHC class II, CD80, and CD86 were not significantly different from those in untreated mice, while that of CD40 was slightly increased. The ability of these DCs to present malaria antigen was evaluated *in vitro* (Fig. 1D). DCs from Flt3L-treated mice stimulated IFN-γ production by malaria-specific $CD8^+$ T cells much better than control DCs, a finding consistent with the increase in the proportion of $CD8^+$ DCs in Flt3L-treated mice (8, 19).

To determine the effect of Flt3L on the pathogenesis of *P. berghei* ANKA infection, Flt3L-treated and untreated mice were infected with *P. berghei* ANKA, and their survival was monitored (Fig. 2A). Most *P. berghei* ANKA-infected control mice died within 8 days with severe symptoms of ECM, such as coma. In contrast, Flt3L-treated mice were clearly protected from lethal CM. Mild symptoms of ECM, such as fur ruffling or hunching, were observed for some of the Flt3L-treated mice within 10 days, but none succumbed to death during this period. The level of parasitemia was significantly reduced in Flt3L-treated mice 5 days after infection with *P. berghei* ANKA but continued to increase to more than 50% within 2 weeks of the infection. The few control mice that survived the critical period of ECM also showed a similar increase in the level of

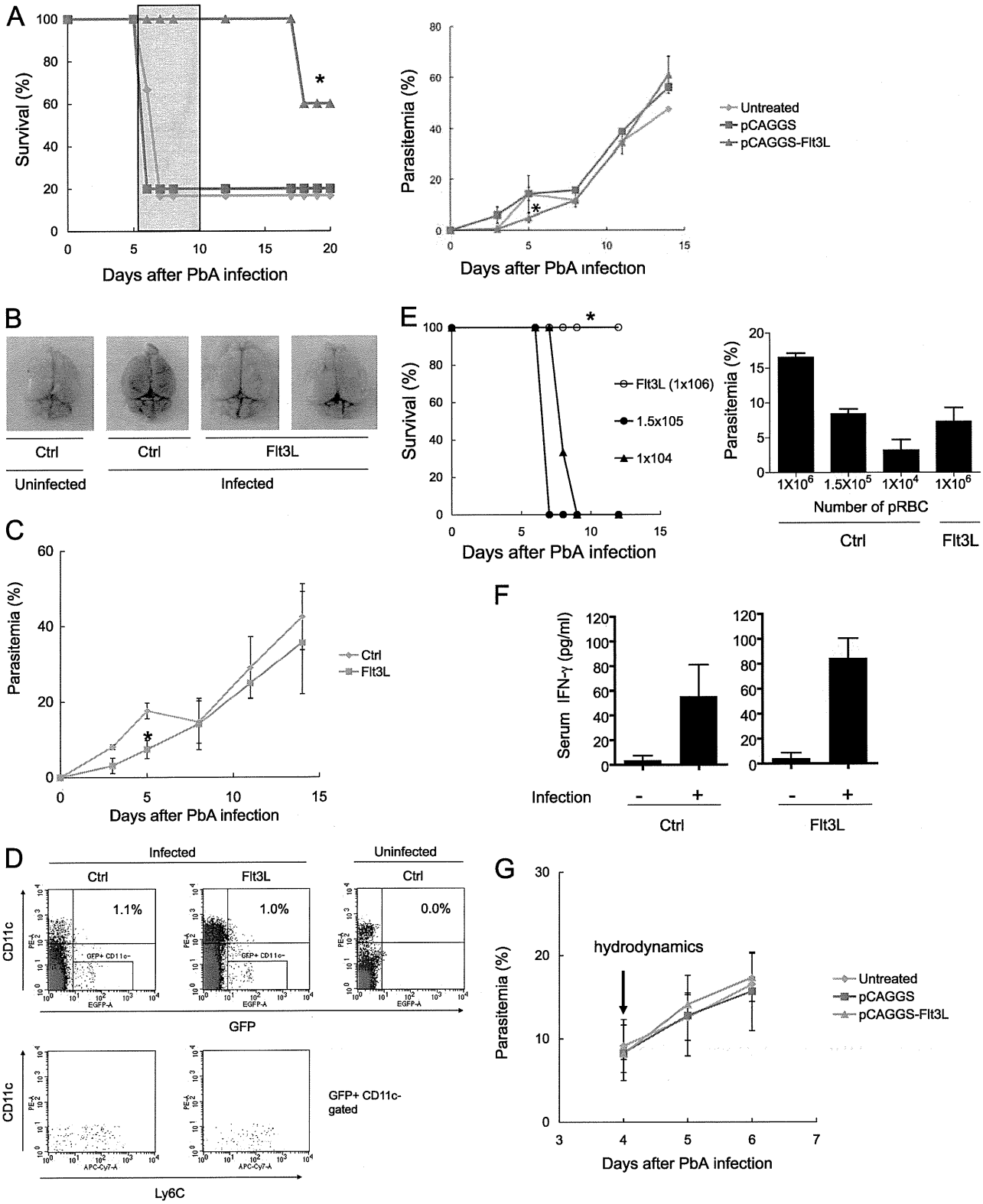

FIG. 2. Flt3L treatment enhanced innate immunity to malaria infection and prevented the development of lethal ECM by mechanisms independent of the reduction of parasitemia. (A) Mice were either left untreated (6 mice) (blue line) or were inoculated with an Flt3L-expressing plasmid (5 mice) (green line) or an empty vector (5 mice) (red line) on day −7 and were infected with pRBC on day 0. (Left) Survival was monitored daily. The green shaded area (days 6 to 10) indicates the dates on which ECM symptoms appear in this disease model in general. The

parasitemia. We tested various doses of the Flt3L plasmid and found an inverse correlation between the number of DCs in the spleen and the levels of parasitemia 5 days after infection (see Fig. S1 in the supplemental material). In addition, mice to which Flt3L-induced DCs were transferred showed reduced parasitemia levels, suggesting that these DCs were directly involved in the antimalaria effects of Flt3L treatment during the early period of the infection (see Fig. S2 in the supplemental material). To visualize the integrity of the blood-brain barrier in infected mice, the leakage of dye in the brain was examined after intravenous (i.v.) injection of Evans blue (Fig. 2B). In control mice, brains were stained with the dye, suggesting that the blood-brain barrier was impaired. However, the brains of Flt3L-treated mice showed little leakage, indicating that the integrity of the blood-brain barrier was maintained. These results suggest that Flt3L treatment effectively prevented the development of ECM.

Since parasitemia levels were inhibited during the early period of the infection in Flt3L-treated mice, we suspected that innate immune responses might be responsible for controlling the parasitemia. To examine this possibility, $Rag2^{-/-}$ mice, which lack both T and B cells, were treated with Flt3L and were infected with *P. berghei* ANKA (Fig. 2C). The levels of parasitemia in Flt3L-treated $Rag2^{-/-}$ mice were lower than those in untreated mice during the early period of the infection, suggesting that enhancement of innate immunity by Flt3L treatment effectively limited the expansion of *P. berghei* ANKA during this period. However, this effect was transient and was not sufficient for protection, since the parasitemia levels continued to rise in infected $Rag2^{-/-}$ mice. Since DCs can phagocytose *Plasmodium*-infected RBC (15), we examined the possibility that Flt3L-expanded DCs phagocytosed pRBC. Flt3L-treated and untreated wild-type C57BL/6 mice were infected with PbA-GFP, and splenocytes were examined 5 days later by using flow cytometry (Fig. 2D). Equivalent proportions of DCs phagocytosed PbA-GFP in Flt3L-treated and untreated mice. In addition to DCs, phagocytosis of PbA-GFP was mediated by a population of $CD11c^{-}$ $Ly6C^{+}$ cells, which are similar to recently described inflammatory monocytes (34).

It is possible that the inhibition of ECM development in Flt3L-treated mice was due to the reduction in parasitemia levels during a critical window for the disease, the early period of infection. To closely examine the relationship between ECM development and parasitemia levels during the early infection period, mice were infected with lower doses of pRBC (Fig. 2E). Although mice infected with 1.5×10^5 pRBC showed parasitemia levels similar to those of Flt3L-treated mice infected with 1×10^6 pRBC, the untreated mice infected with the lower pRBC dose did develop lethal CM. Since IFN-γ plays a critical role in the pathogenesis of ECM (40), we determined serum IFN-γ levels in Flt3L-treated and untreated mice during infection (Fig. 2F). The level of IFN-γ was slightly higher in Flt3L-treated mice than in untreated mice after *P. berghei* ANKA infection. To exclude the possibility that Flt3L directly inhibited parasite growth, we examined the effect of Flt3L on the growth of *P. berghei* ANKA *in vivo* prior to the expansion of DCs. Thus, we treated mice with Flt3L 4 days after infection (Fig. 2G). Two days after Flt3L treatment, when serum Flt3L levels had significantly increased (1.71 ± 0.79 ng/ml in treated mice versus 0.32 ± 0.02 ng/ml in untreated mice), the parasitemia level was not reduced, suggesting that Flt3L did not directly inhibit parasite growth. Taking these data together, we concluded that it was unlikely that inhibition of ECM development in Flt3L-treated mice was due simply to the inhibition of parasitemia or to the change in the systemic IFN-γ response.

Expansion and activation of $CD8^{+}$ T cells in Flt3L-treated *P. berghei* ANKA-infected mice. Since ECM is a T cell-dependent disease, we next examined the number and phenotype of T cells 5 days after infection with *P. berghei* ANKA. The numbers of $CD4^{+}$ and $CD8^{+}$ T cells did not change significantly after infection of untreated mice with *P. berghei* ANKA but increased dramatically in both the spleen and peripheral blood after infection of Flt3L-treated mice with *P. berghei* ANKA (Fig. 3A). In particular, the increase in the number of $CD8^{+}$ T cells was prominent. To investigate the function of these $CD8^{+}$ T cells, they were stimulated with DCs pulsed with a pRBC lysate. $CD8^{+}$ T cells from Flt3L-treated mice produced IFN-γ in response to malaria antigen at levels similar to or higher than those from untreated mice, suggesting that the priming and IFN-γ production of $CD8^{+}$ T cells specific for malaria antigen were not impaired in Flt3L-treated mice (Fig. 3B).

We next examined the phenotypes of $CD8^{+}$ T cells, since they are critical for the pathogenesis of ECM. Interestingly, a large population of $CD8^{+}$ T cells was found to express CD11c in mice infected with *P. berghei* ANKA, while CD11c was not

asterisk indicates a significant difference between untreated or empty-vector-treated mice and pCAGGS-Flt3L-treated mice (P, <0.05 by the log rank test). (Right) Parasitemia was monitored every 2 to 3 days in surviving mice, and the mean ± SD for each group is shown. The asterisk indicates a significant difference between untreated or empty-vector-treated mice and Flt3L-treated mice (P, <0.05 by the Mann-Whitney test). (B) Six days after infection with *P. berghei* ANKA, the integrity of the blood-brain barrier was evaluated by injection of Evans blue solution. (C) $Rag2^{-/-}$ mice were either left untreated (6 mice) (blue line) or treated with Flt3L (5 mice) (green line) and were infected with pRBC 7 days later. The parasitemia level was monitored every 2 to 3 days, and the mean ± SD for each group is shown. The asterisk indicates a significant difference between untreated and Flt3L-treated mice (P, <0.05 by the Mann-Whitney test). (D) Untreated or Flt3L-treated B6 mice were infected with PbA-GFP. Five days after infection, spleen cells were analyzed using flow cytometry. (Top) The percentage of GFP^{+} cells within $CD11c^{high}$ DCs is given in the upper right corner. (Bottom) The expression of Ly6C within GFP^{+} $CD11c^{-}$ cells is shown. (E) Mice (3 mice/group) were infected with the indicated number of pRBC. (Left) Survival was monitored daily. The asterisk indicates a significant difference ($P < 0.05$) by the log rank test. (Right) The levels of parasitemia 5 days after infection are expressed as means ± SD. (F) Sera were collected from untreated (Ctrl) or Flt3L-treated mice (3 mice/group) 5 days after *P. berghei* ANKA infection and were subjected to a CBA assay. The mean ± SD for each group is shown. (G) Mice (3 mice each in the Flt3L and pCAGGS groups; 5 mice in the untreated group) were infected with *P. berghei* ANKA and were either left untreated (blue line) or inoculated with an Flt3L-expressing plasmid (green line) or an empty vector (red line) on day 4. The levels of parasitemia were monitored, and the mean ± SD for each group was determined. Experiments for which results are shown in panels A to D and F were repeated twice, and representative data are shown.